Surface Mass Loading of the Solid Earth: Theory and Examples

T. van Dam, University of Luxembourg

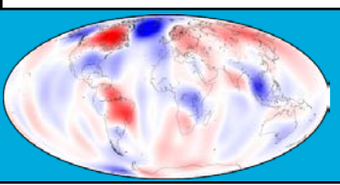

Outline

1. Introduction
2. Method for calculating the elastic loading effects on an elastic Earth model
   - Love numbers
   - Green's functions approach
   - Spherical harmonics approach
3. Determining the response of an elastic Earth to atmospheric loading
4. Loading effects of continental water storage
5. Loading effects of ocean bottom pressure
6. Total Load

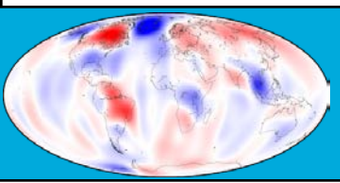

1. Introduction

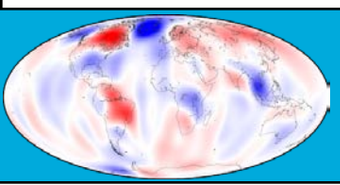

1. Introduction

- What is surface mass loading?

Surface mass loading includes all the masses above the Earth's surface. However, we focus on these surface mass loadings which induce elastic response of the Earth's crust, e.g. atmosphere, ocean and continental water (hydrology).

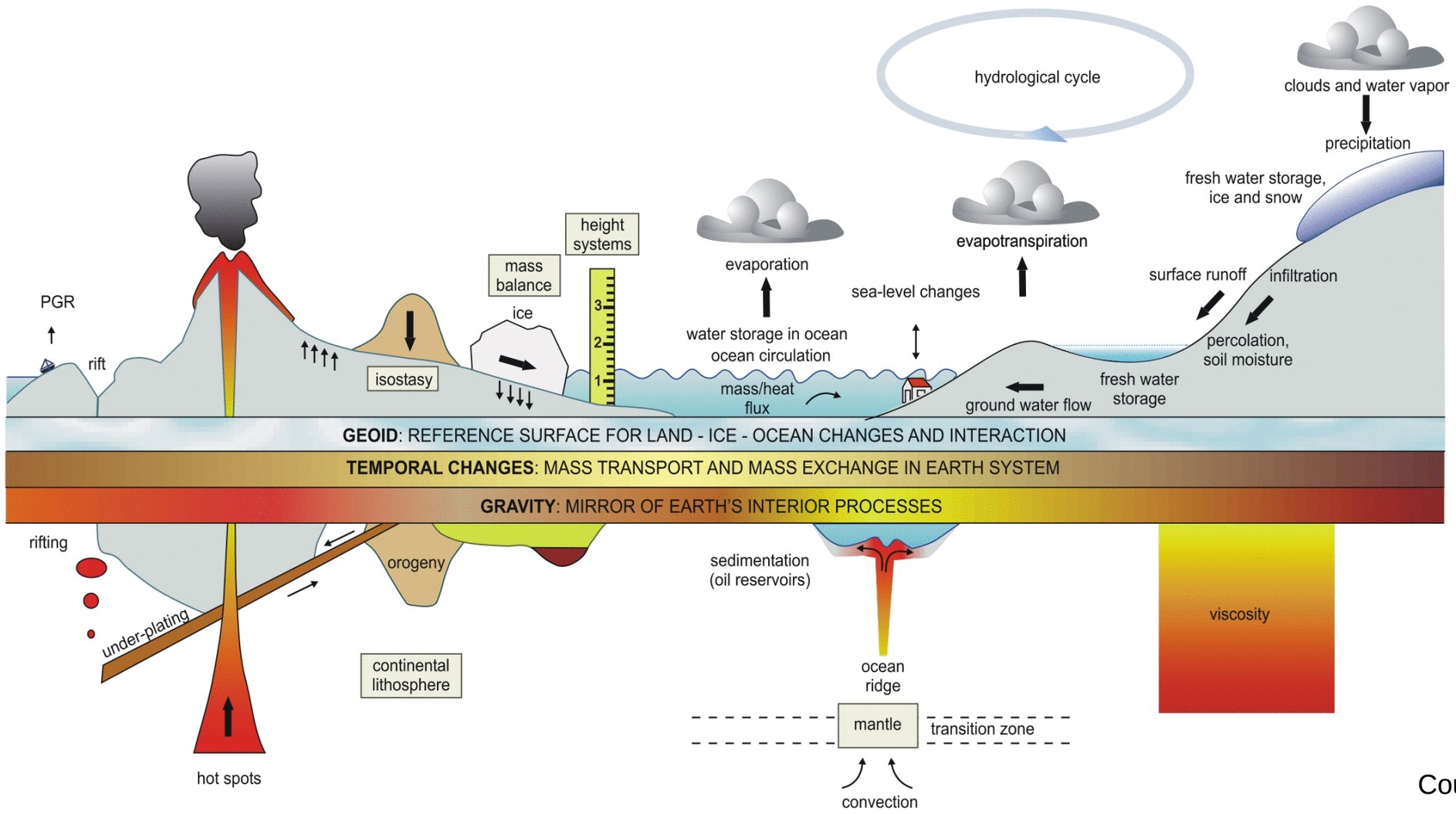

Coutesy: Ilk et al. (2005)

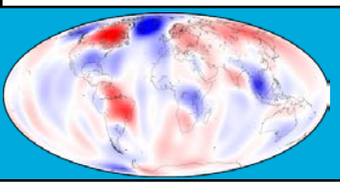

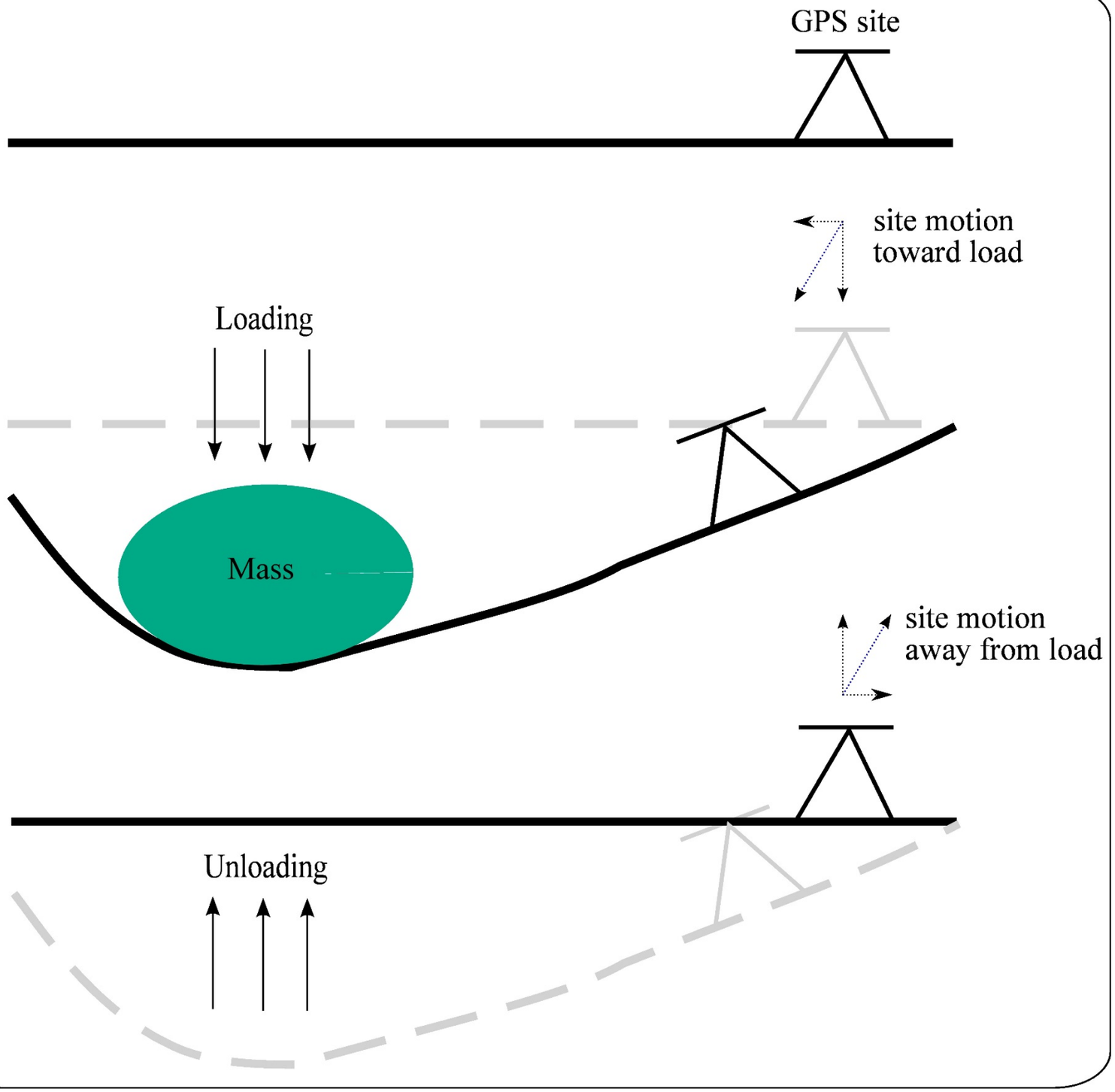

- Example of elastic loading and unloading

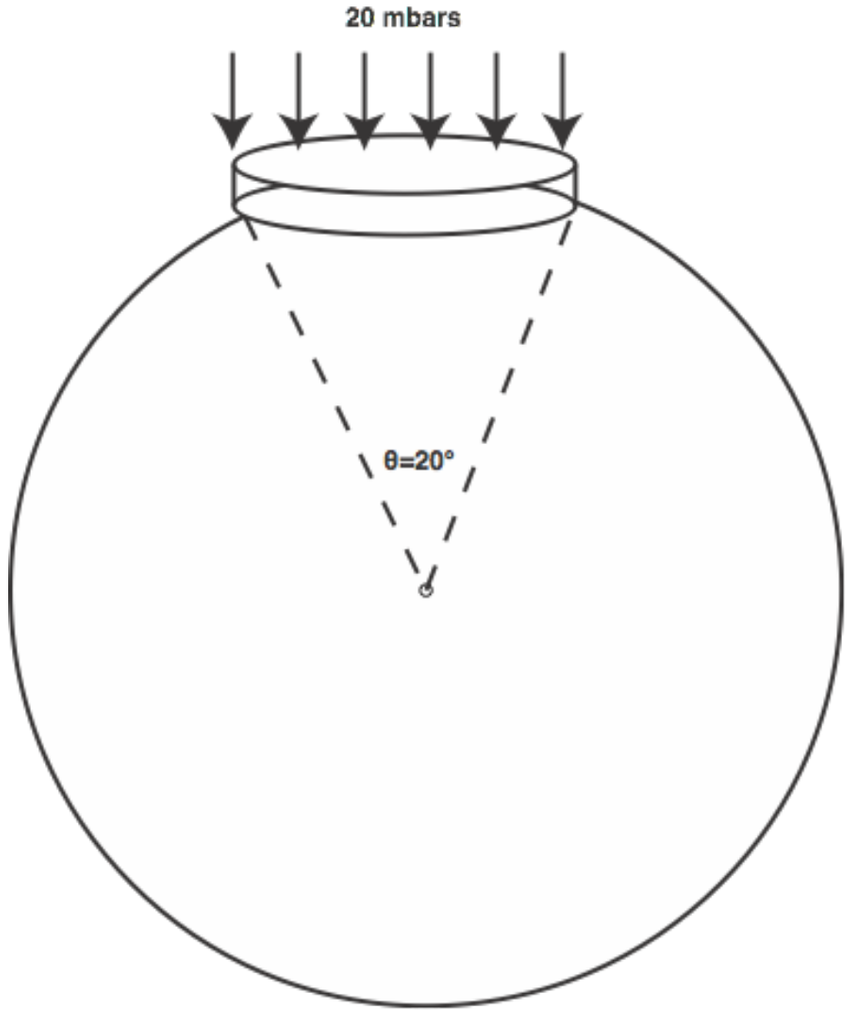

- uniform mass increase of 20 millibars
- disk of diameter 2000 km or angular extent of 20º
- produces a depression of 1 cm at the center of the disk

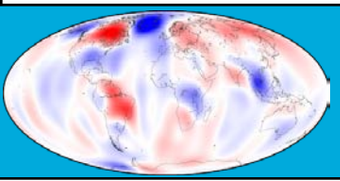

2. Method for calculating the elastic loading effects on an elastic Earth model

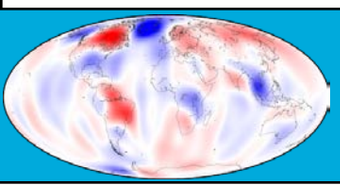

Love Numbers

- The Love h and k, and Shida l numbers were firstly introduced by Love (1909) and Shida and Matsuyama (1912), respectively to characterize the Earth's response to the potential or force without loading the surface of the Earth, such as the external tidal potential
- For describing the response to the surface load, e.g. terrestrial water load, another type of Love numbers distinguished by a superscript prime, i.e. h', l' and k', were adopted, which are normally called loading Love numbers (Farrell, 1972).
- The elastic loading Love numbers are computed by integrating the equations of motion, the stress-strain relationship and Poisson equation inside the Earth, from the center to the surface using a spherical Earth model, e.g. the Preliminary Reference Earth Model (PREM)

Farrell, W.E., Deformation of the Earth by surface loads, Rev. of Geophys. and Space Phys., 10, 761-797, 1972.

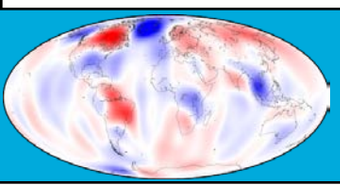

- The equations of motion as well as the Poisson equation are linearized and formulated as follows (Farrell, 1972):

$$\nabla \cdot \boldsymbol{\tau} - \nabla(\rho g \mathbf{s} \cdot \mathbf{e_r}) - \rho \nabla \phi + g \nabla \cdot (\rho \mathbf{s} \mathbf{e_r}) = 0\,, \qquad \text{2.1a}$$

$$\nabla^2 \phi = -4\pi G \nabla \cdot (\rho \mathbf{s})\,, \qquad \text{2.1b}$$

where $\boldsymbol{\tau}$ is the incremental stress tensor

ρ and g are the unperturbed density and gravitational acceleration

$\mathbf{s}$ is the displacement vector

ϕ is the perturbed gravitational potential

$\mathbf{e_r}$ denotes the unit vector of the vertical component.

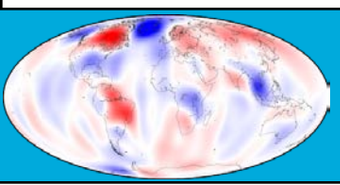

- Supposing a spherically symmetric Earth model with certain boundary conditions at the surface, the solutions of Eq. 2.1a and Eq. 2.1b can be transformed and expressed as

$$\mathbf{s} = \sum_{n=0}^{\infty} \left(U_n(r) P_n(\cos\psi)\mathbf{e_r} + V_n(r) \frac{\partial P_n(\cos\psi)}{\partial \psi} \mathbf{e_v} \right) , \qquad 2.2a$$

$$\phi = \sum_{n=0}^{\infty} \Phi_n(r) P_n(\cos\psi) , \qquad 2.2b$$

where U_n, V_n and Φ_n are transformed variables indicating vertical displacements, tangential displacements and potential, respectively. $\mathbf{e_v}$ denotes the unit vector of the horizontal component.

- With further simplifications applied, the transformed variables can be further related to the elastic loading Love numbers

$$\begin{bmatrix} U_n(r) \\ V_n(r) \\ \Phi_n(r) \end{bmatrix} = W(r) \begin{bmatrix} h'_n(r)/g \\ l'_n(r)/g \\ k'_n(r) \end{bmatrix} , \qquad 2.3$$

where $W(r)$ stands for the potential induced by the point mass

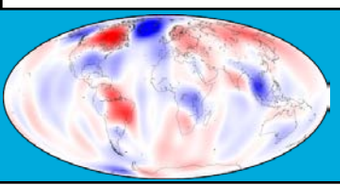

- Solving and integrating Eq. 2.3 from the inner Earth to the surface gives the set of loading Love numbers which are based on the given Earth model.
- Five different sets of elastic loading Love Numbers come from five different Earth models

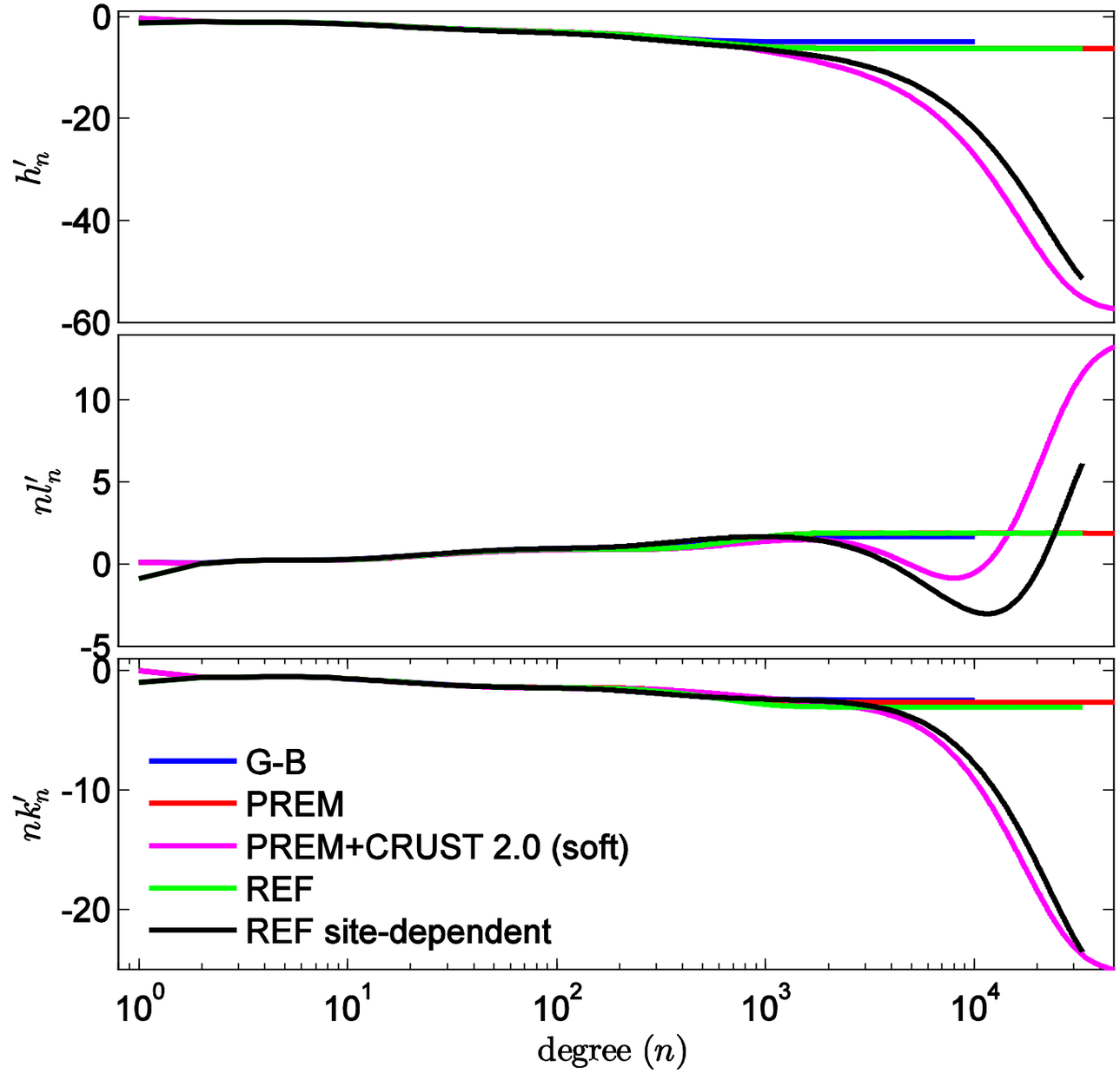

1) Gutenberg-Bullen (Farrell, 1972);
2) PREM (Dziewonski and Anderson, 1981);
3) a modified PREM with crustal structures adapting from CRUST 2.0 model (Wang et al., 2012)
4) REF (Kustowski et al., 2008)
5) REF model with a site-dependent setting (Gegout, 2013).

Gegout P. et al. (2010). Practical numerical computation of Lover numbers and applications.

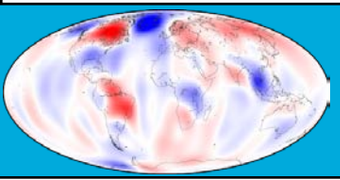

Green's Functions Approach

- The analysis of the deformation of an elastic solid is a classic problem in geophysics and is discussed in numerous books and papers.

- Solutions to the momentum equations have been formulated to describe the deformations of the Earth due to mass loading of its surface (Longman[1], 1962; Farrell[2], 1972)

- For a detailed review of the subject please see the paper by Farrell.

[1]Longman, I.M., A Green's function for determining the deformation fo the Earth due to surface mass loads, 1, Theory, JGR, 67, 845, 1962.
[2]Farrell, W.E., Deformation of the Earth by surface loads, Rev. of Geophys. and Space Phys., 10, 761-797, 1972.

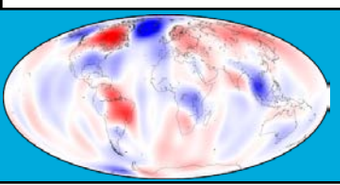

- Consider a point element of mass, dM, located at r' on the Earth's surface

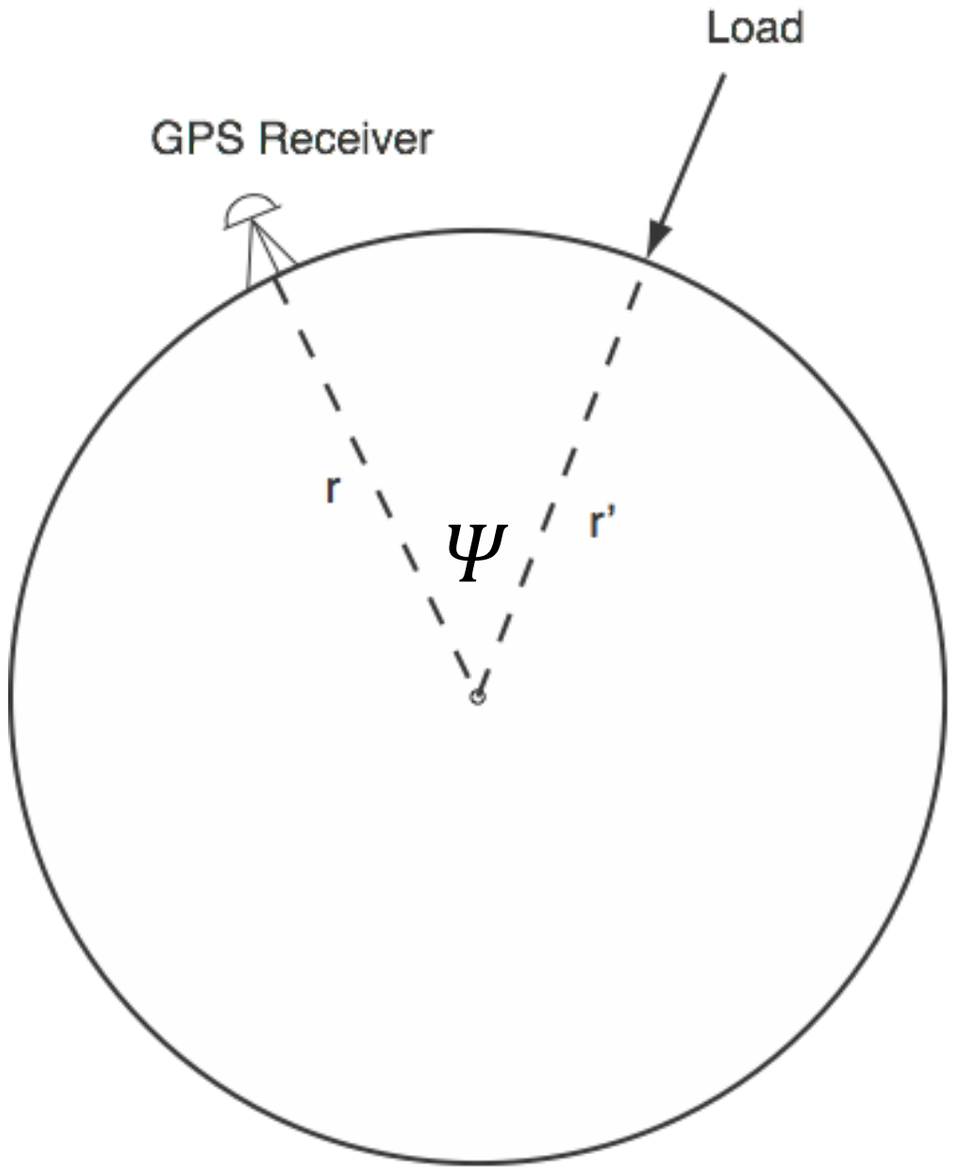

- Substituting Eq. 2.3 into Eq. 2.2, one can obtain the elastic Green functions for the radial (u_r) and tangential (u_t) displacements evaluated at the Earth's surface,

$$G = G_{u_r} = \frac{R}{M}\sum_{n=0}^{\infty} h'_n P_n(\cos\Psi) \qquad 2.4a$$

$$G = G_{u_t} = \frac{R}{M}\sum_{n=1}^{\infty} l'_n \frac{\partial}{\partial\Psi} P_n(\cos\Psi) \qquad 2.4b$$

- The load Love numbers, h'_n ,$l'_n$and k'_n ,become constant, h'_∞ ,$l'_\infty$and k'_∞ , at large n

- The Green's functions can be written as (see Farrell, 1972)

$$G_{u_r} = \frac{R}{M} h'_\infty \sum_{n=0}^{\infty} P_n(\cos\Psi) + \frac{R}{M}\sum_{n=0}^{\infty}(h'_n - h'_\infty) P_n(\cos\Psi) \qquad 2.5a$$

$$G_{u_t} = \frac{R}{M} l'_\infty \sum_{n=1}^{\infty} \frac{1}{n}\frac{\partial}{\partial\Psi} P_n(\cos\Psi) + \frac{R}{M}\sum_{n=1}^{\infty}(n l'_n - l'_\infty)\frac{1}{n}\frac{\partial}{\partial\Psi} P_n(\cos\Psi) \qquad 2.5b$$

- The first summation in both expressions can be expressed analytically by Kummer's transformation

$$G_{u_r} = \frac{R}{2M}\frac{h'_\infty}{\sin(\Psi/2)} + \frac{R}{M}\sum_{n=0}^{\infty}(h'_n - h'_\infty)P_n(\cos\Psi) \qquad 2.6a$$

$$G_{u_t} = -\frac{R}{M}l'_\infty\frac{\cos(\Psi/2)[1+2\sin(\Psi/2)]}{2\sin(\Psi/2)[1+\sin(\Psi/2)]} + \frac{R}{M}\sum_{n=1}^{\infty}(nl'_n - l'_\infty)\frac{1}{n}\frac{\partial}{\partial\Psi}P_n(\cos\Psi) \qquad 2.6b$$

- only a finite number of terms are required to evaluate the second summations in these expressions
- Green's functions are computed for various Earth models

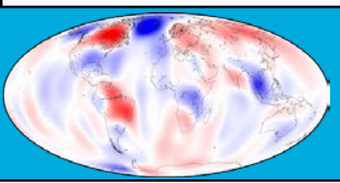

- Green's functions from different Earth models

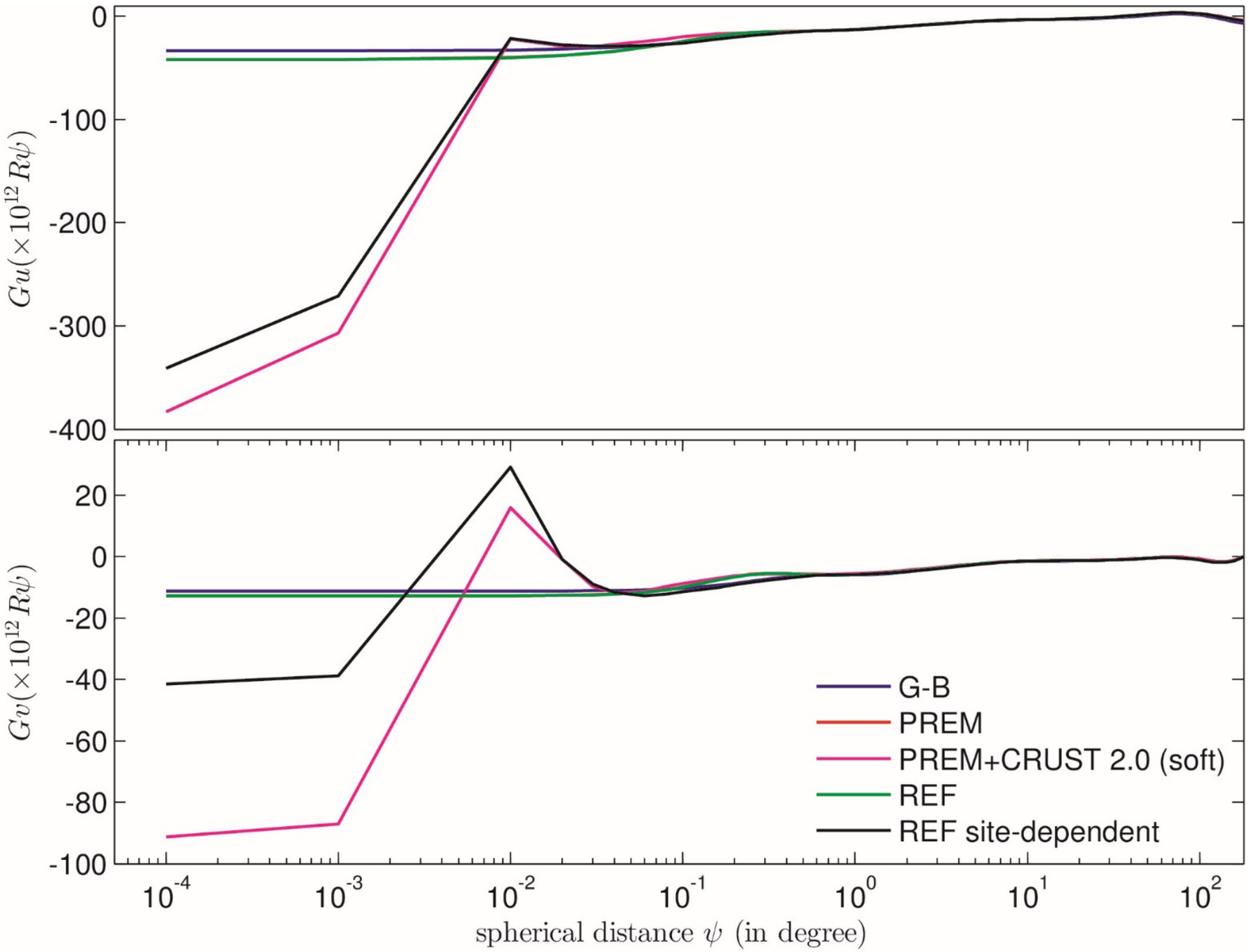

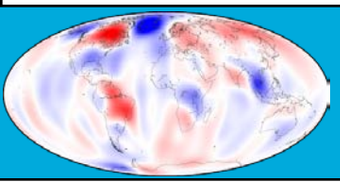

Computing the load at a point due to a point load at Ψ

- recall that given a certain Earth model, that the Green's function tells you how the surface is displaced at your GPS receiver give a 1 kg load at Ψ
- let's look at the radial displacement $dU = G(\Psi)dM$
- if the load is separated from the receiver by $20°$, $G(20°) = 2.619/(10^{12} \times a \times \Psi)$ *(Farrell's Green's Functions are normalized for a 1 kg load)*
- $a = 6.371 \times 10^6$ m
- $\Psi = 20° = 0.3491$ (in radians)
- $dU = 2.619/(10^{12} \times a \times \Psi)$
- $dU = 2.619/(10^{12} \times (6.371 \times 10^6) \times 0.3491)$
- $dU = 0.11 \times 10^{-19}$ meters
- loads need to be big to induce a displacement of the Earth's surface

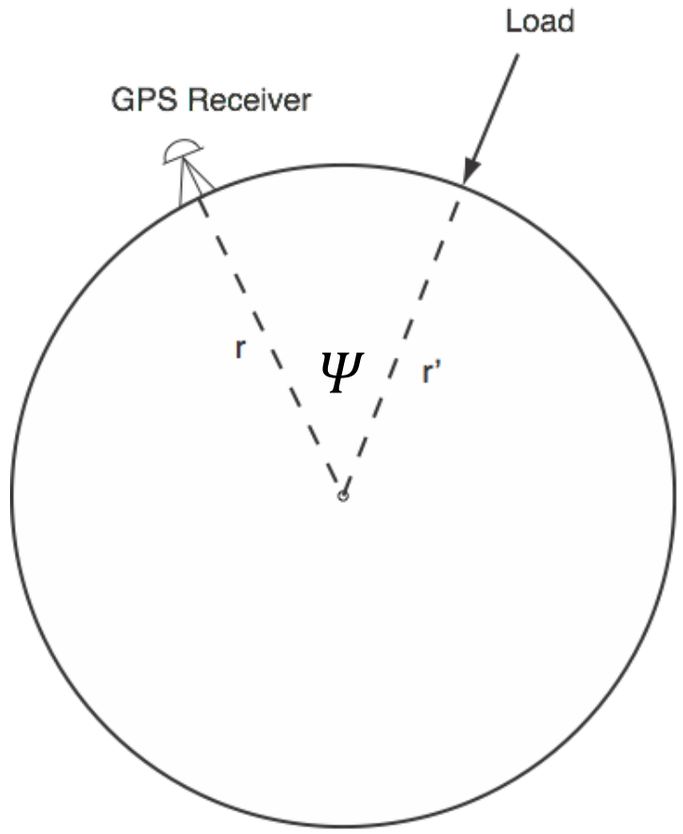

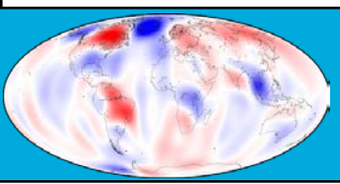

Spatial convolution over the loading area

- Supposing we evaluate the deformations at any point *P* with colatitude θ_P and longitude ϕ_P due to the surface mass load dM at point *Q* with colatitude θ_Q and longitude ϕ_Q, convolving the load mass and Green's functions leads to vertical displacement du_r and north du_n and east displacement du_e

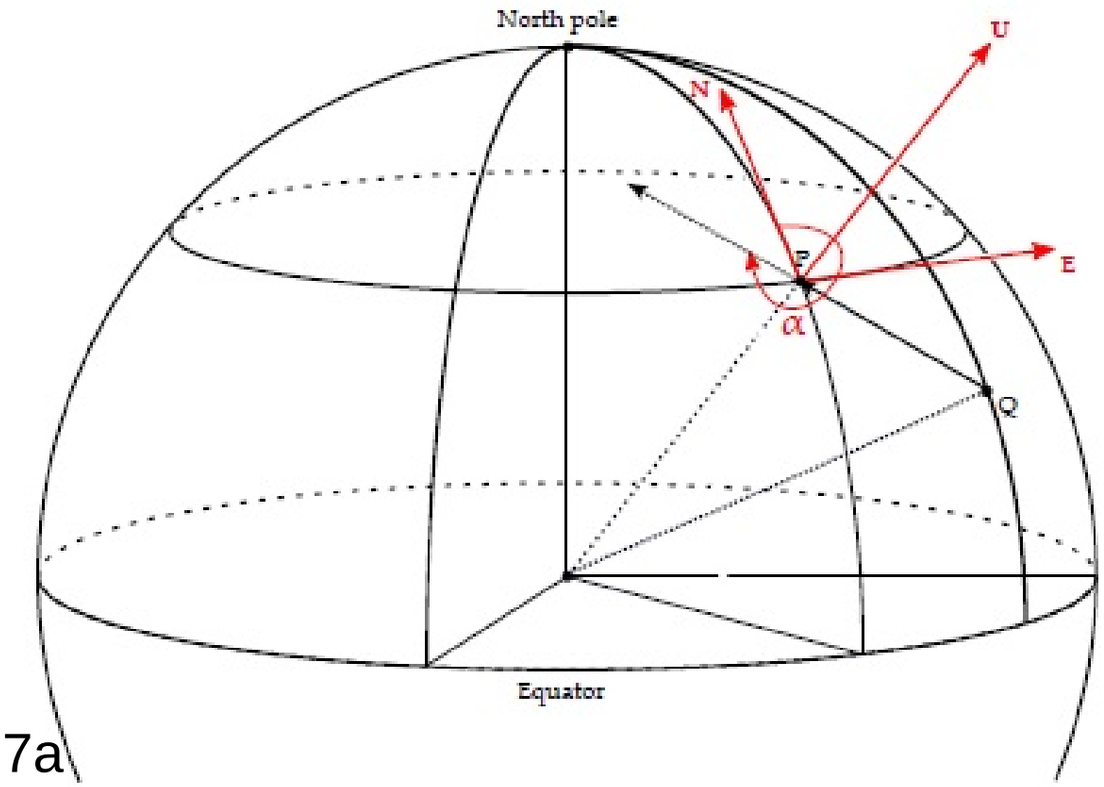

$$du_r(\theta_P, \phi_P) = a^2 \iint_\Omega G_{u_r}(\Psi_{PQ}) dM_Q d\Omega \quad 2.7a$$

$$du_n(\theta_P, \phi_P) = -a^2 \cos\alpha \iint_\Omega G_{u_t}(\Psi_{PQ}) dM_Q d\Omega \quad 2.7b$$

$$du_e(\theta_P, \phi_P) = -a^2 \sin\alpha \iint_\Omega G_{u_t}(\Psi_{PQ}) dM_Q d\Omega \quad 2.7c$$

where $d\Omega = \sin\theta_Q d\theta_Q d\phi_Q$ and $a^2 d\Omega$ gives the surface area of the corresponding surface load

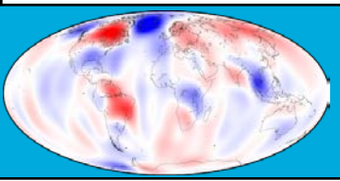

- let's say the mass is 10^{-2} kg/cm^2 and that it extends over a disk of varying degrees

$$dU = 2\pi[(6.371)^2 \times 10^{16}] \times 10^{-2} \times \frac{10^2}{6.371 \times 10^{18}} \int_0^{\theta_0} \frac{G_0(\theta)\sin\theta}{\theta} d\theta$$

$\int d\phi$ a^2 dM Green's function Normalization and converting from m to cm

- for all $\theta \leq \theta_0, \sin\theta/\theta = 1$
- $G_0(\theta)$ are the numbers from Table A3 in Farrell
- For a disk load of 20 degrees loaded by a mass/area of 10^{-2} kg/cm, the Earth under the center of the load is displaced by 0.67 cm toward the center of the Earth

θ (deg)	dU (cm)
1	-0.12
2	-0.19
4	-0.29
6	-0.36
8	-0.42
10	-0.47
20	-0.67

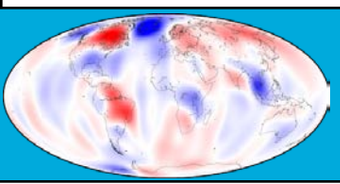

Spherical harmonic Approach: from spatial to spectral

- Instead of spatial convolution, we can express surface mass variations in terms of spherical harmonics

$$\Delta\sigma(\theta,\lambda) = R\rho_{\mathrm{w}} \sum_{n=0}^{\infty} \sum_{m=0}^{n} \bar{P}_{nm}(\cos\theta)\left(\Delta\bar{C}^{\sigma}_{nm}\cos m\lambda + \Delta\bar{S}^{\sigma}_{nm}\sin m\lambda\right) \qquad 2.8$$

where $\Delta\sigma(\theta,\lambda)$ represents surface mass density changes and $\overline{P}_{nm}$ is the normalized Legendre functions of the spectral degree n and order m, $\Delta\overline{C}^{\sigma}_{nm}$ and $\Delta\overline{S}^{\sigma}_{nm}$ are fully normalized dimensionless spherical harmonic coefficients indicating surface mass density changes.

- Two more important equations

$$\begin{Bmatrix} \Delta\bar{C}^{\sigma}_{nm} \\ \Delta\bar{S}^{\sigma}_{nm} \end{Bmatrix} = \frac{\rho_{\mathrm{e}}}{3\rho_{\mathrm{w}}} \frac{2n+1}{1+k'_n} \begin{Bmatrix} \Delta\bar{C}_{nm} \\ \Delta\bar{S}_{nm} \end{Bmatrix}$$

Relationship between mass density spherical harmonics and gravity spherical harmonics

2.9

Global spherical harmonic analysis

$$\begin{Bmatrix} \Delta\bar{C}^{\sigma}_{nm} \\ \Delta\bar{S}^{\sigma}_{nm} \end{Bmatrix} = \frac{1}{4\pi R\rho_{\mathrm{w}}} \iint \Delta\sigma(\theta,\lambda)\bar{P}_{nm} \begin{Bmatrix} \cos(m\lambda) \\ \sin(m\lambda) \end{Bmatrix} d\Omega$$

2.10

Wahr J. et al. (1998), Time variability of the Earth's gravity field: Hydrological and oceanic effects and their possible detection using GRACE. JGR, 103(B12):30
Chen Q (2015), Analyzing and modeling environmental loading induced displacements with GPS and GRACE, PhD thesis, Uni Stuttgart

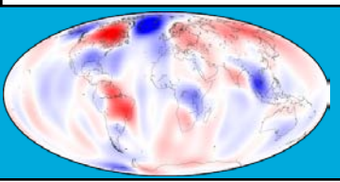

Spherical harmonic Approach

- By applying the addition theorem

$$P_n(\cos\psi_{PQ}) = \frac{1}{2n+1}\sum_{m=0}^{n}\bar{P}_{nm}(\cos\theta_P)\bar{P}_{nm}(\cos\theta_Q)\cos m(\lambda_P-\lambda_Q) \qquad 2.11$$

to the Green's function equation 2.4, we can get

$$G_u(\psi_{PQ}) = \frac{R}{M}\sum_{n=0}^{\infty}\frac{h'_n}{2n+1}\sum_{m=0}^{n}\bar{P}_{nm}(\cos\theta_P)\bar{P}_{nm}(\cos\theta_Q)\cos m(\lambda_P-\lambda_Q) \qquad 2.12$$

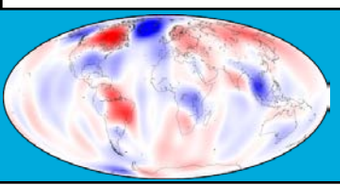

Spherical harmonic Approach

- Inserting the equation 2.12 into 2.7a together with equations 2.8 and 2.10, we get

$$d_{u_r}(\theta_P,\phi_P) = \frac{a^3}{M}\iint \Delta\sigma(\theta_Q,\phi_Q)\sum_{l=0}^{\infty}\frac{h'_l}{2l+1}\sum_{m=0}^{l}(\tilde{P}_{lm}(\cos\theta_P)\tilde{P}_{lm}(\cos\theta_Q)\cos m\phi_P\cos m\phi_Q$$

$$+\tilde{P}_{lm}(\cos\theta_P)\tilde{P}_{lm}(\cos\theta_Q)\sin m\phi_P\sin m\phi_Q)d\Omega$$

$$=\frac{a^3}{M}\sum_{l=0}^{\infty}\frac{h'_l}{2l+1}\sum_{m=0}^{l}\iint \Delta\sigma(\theta_Q,\phi_Q)(\tilde{P}_{lm}(\cos\theta_P)\tilde{P}_{lm}(\cos\theta_Q)\cos m\phi_P\cos m\phi_Q$$

$$+\tilde{P}_{lm}(\cos\theta_P)\tilde{P}_{lm}(\cos\theta_Q)\sin m\phi_P\sin m\phi_Q)d\Omega$$

$$=\frac{a^3}{M}\sum_{l=0}^{\infty}4\pi R\rho_w\frac{h'_l}{2l+1}\sum_{m=0}^{l}(\tilde{P}_{lm}(\cos\theta_P)\cos m\phi_P\Delta\hat{C}_{lm}$$

$$+\tilde{P}_{lm}(\cos\theta_P)\sin m\phi_P\Delta\hat{S}_{lm})$$

$$=\frac{3a\rho_w}{\rho_e}\sum_{l=0}^{\infty}\frac{h'_l}{2l+1}\sum_{m=0}^{l}(\tilde{P}_{lm}(\cos\theta_P)\cos m\phi_P\Delta\hat{C}_{lm}$$

$$+\tilde{P}_{lm}(\cos\theta_P)\sin m\phi_P\Delta\hat{S}_{lm})$$

2.13

Computing loading induced displacements from gravity SHs.

- Finally, applying the equation 2.9 to the above equations, we can get

$$d_u(\theta_P,\lambda_P) = R\sum_{n=1}^{\infty}\frac{h'_n}{1+k'_n}\sum_{m=0}^{n}\bar{P}_{nm}(\cos\theta_P)(\Delta\bar{C}_{nm}\cos m\lambda_P+\Delta\bar{S}_{nm}\sin m\lambda_P)$$

2.14

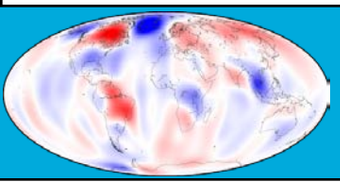

- Convolution in both the spatial and spectral domain is mathematically equivalent. But practically, difference between them exists.

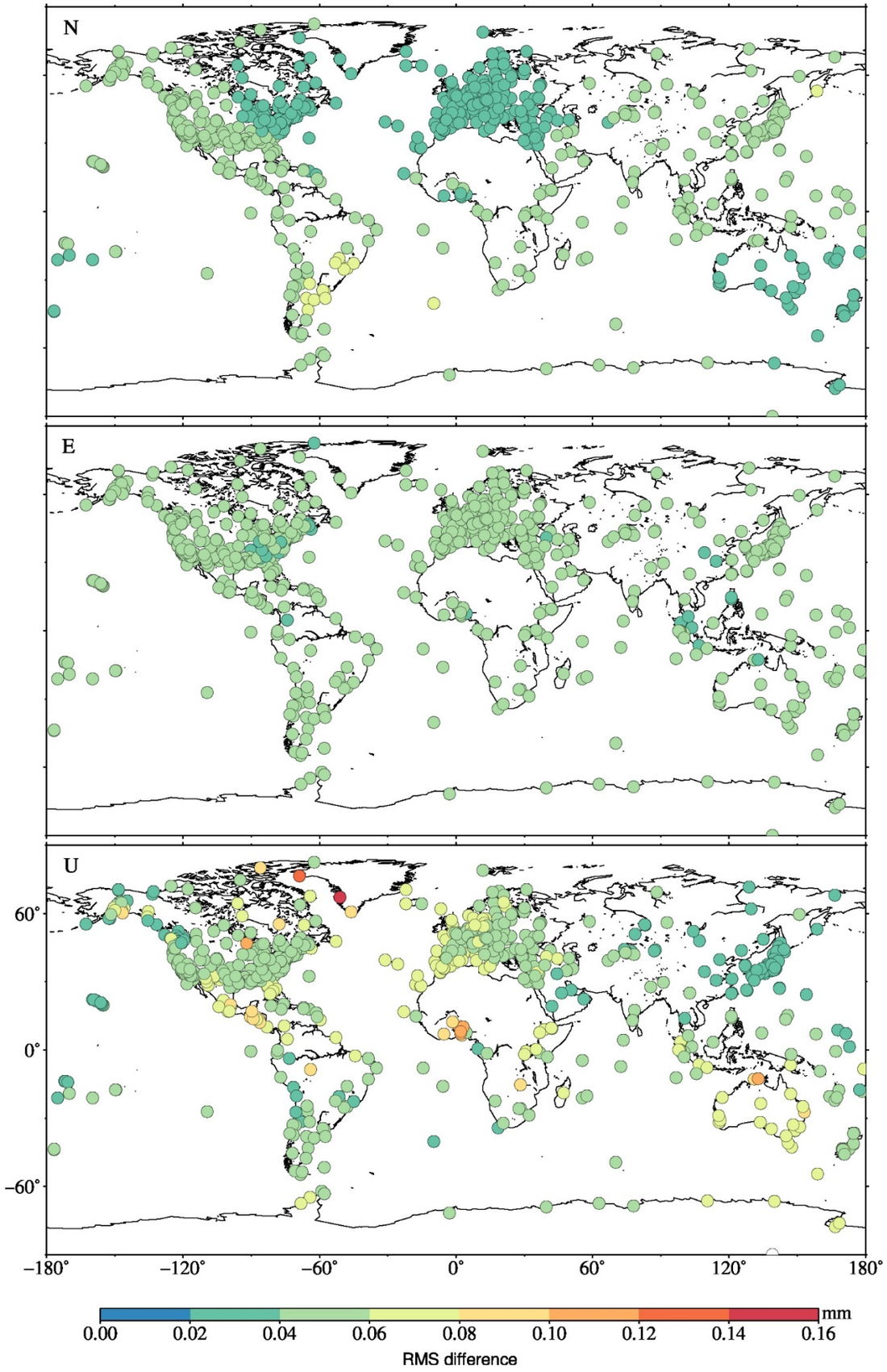

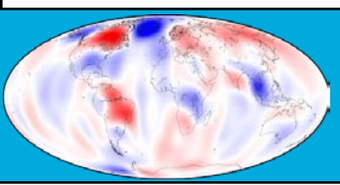

3. Atmospheric Pressure Loading

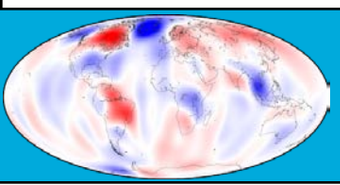

3. Atmospheric Pressure Loading

- Surface pressure deviations from average sea level pressure, 1000 mbars, 24-06-2010
- zero mbars over the oceans, sea-level
- low pressure over Antarctica and mountains

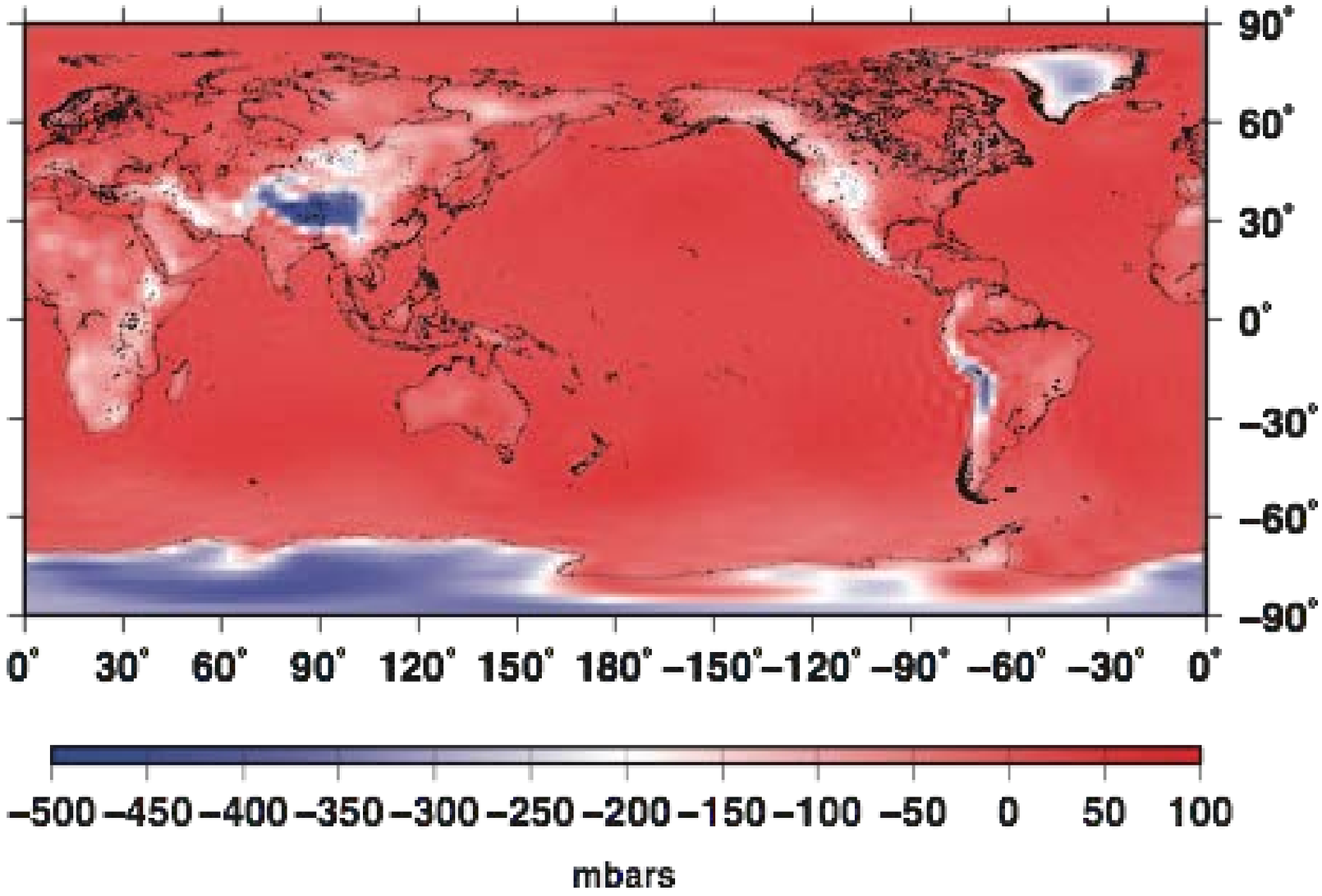

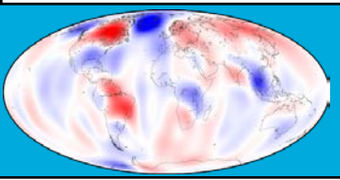

- Longest period, annual
- 10 years of surface pressure data, 2000-2010, NCEP
  - remove mean
  - fit: $y = b + mx$
    $+ A \sin \omega t + B \cos \omega t$

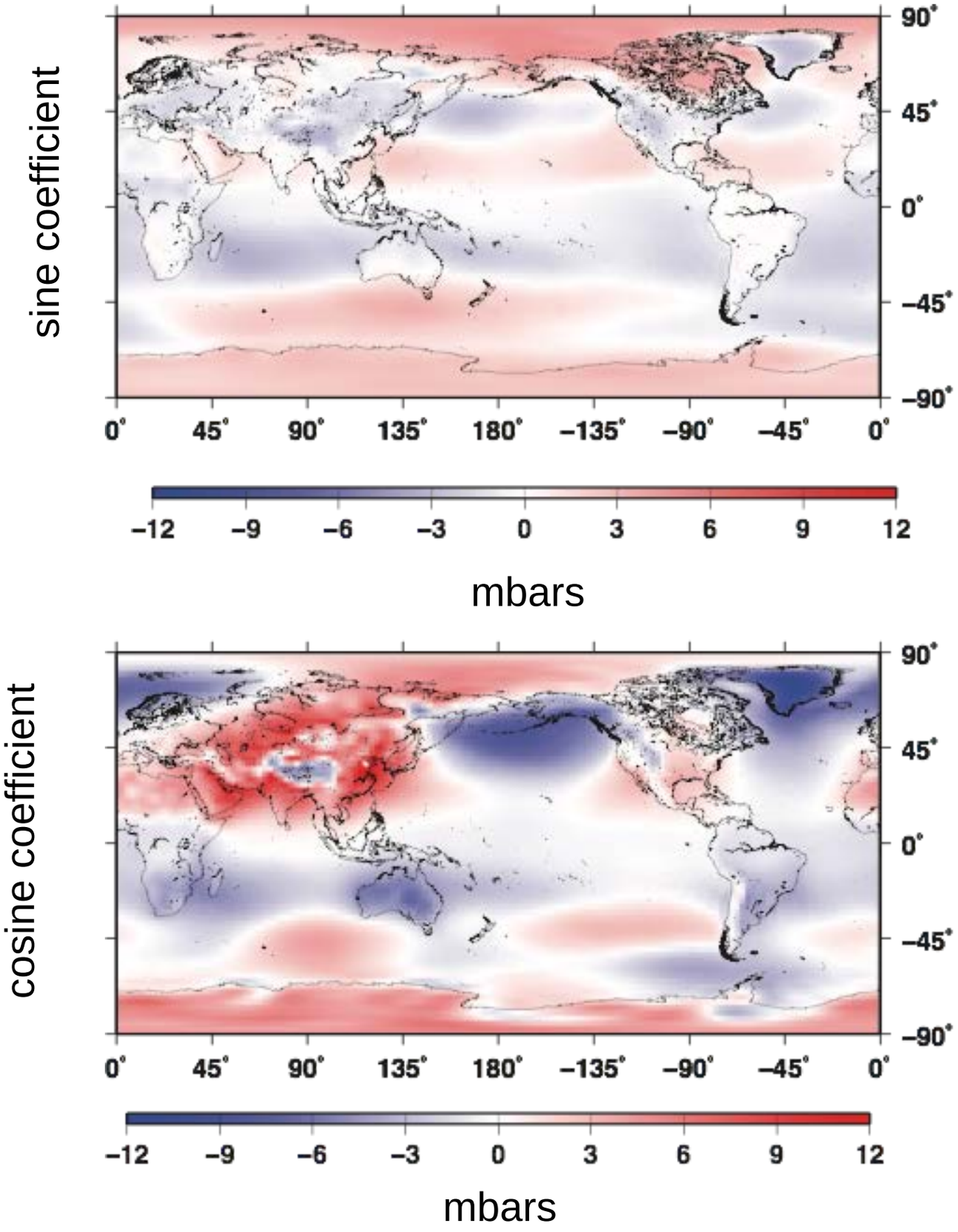

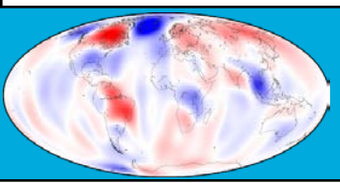

- Atmospheric pressure from the winter versus the summer

Average winter

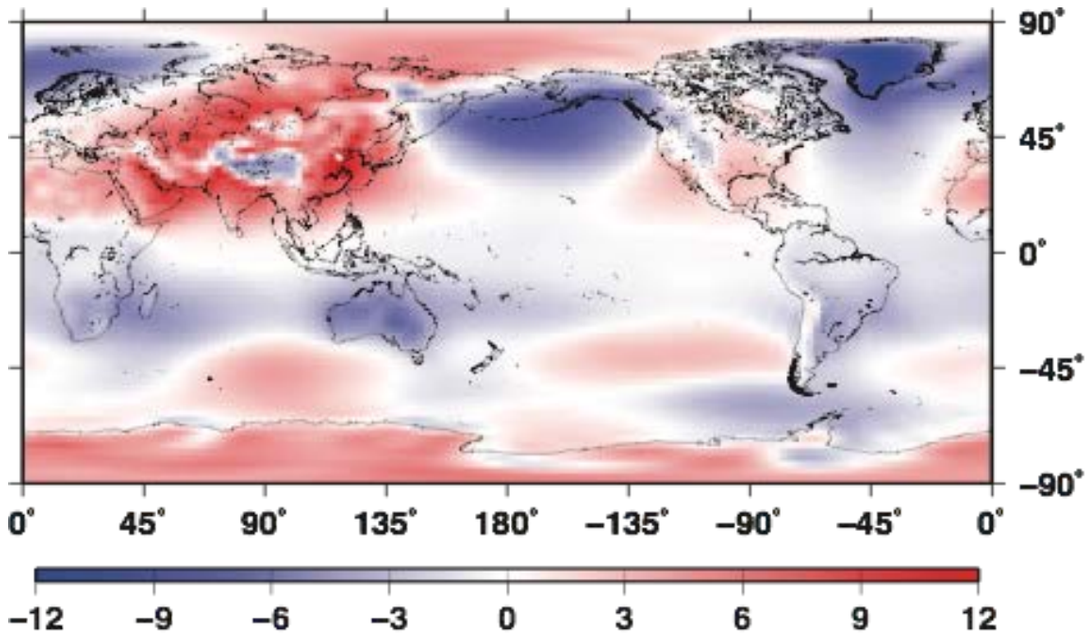

mbar

Average summer

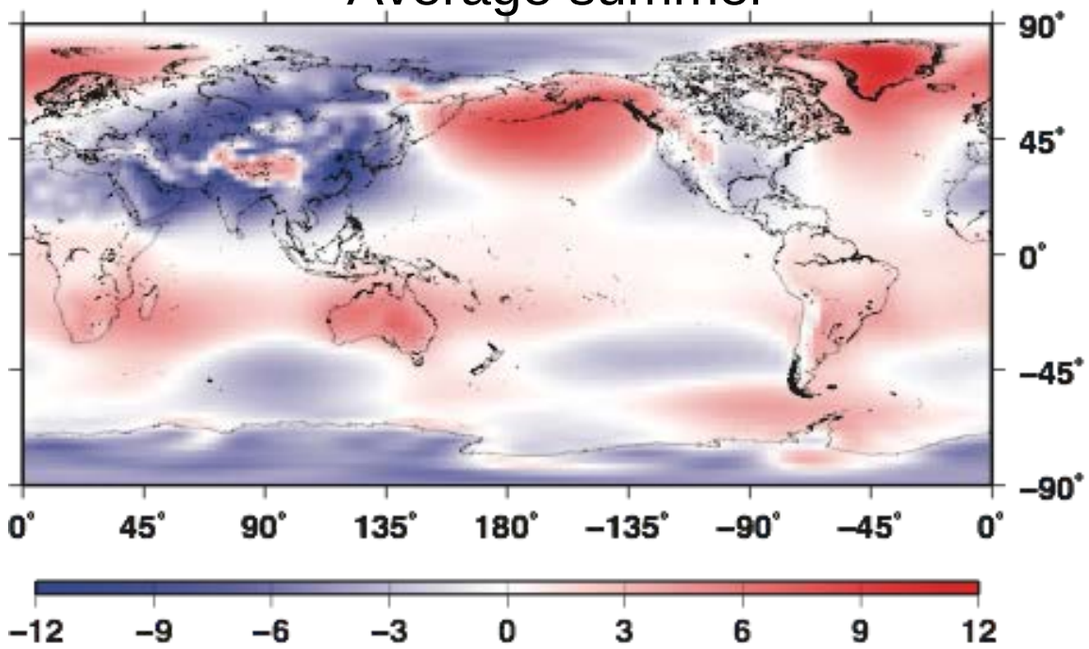

mbar

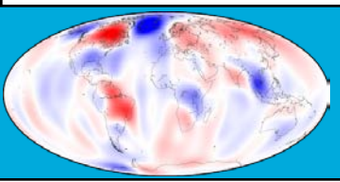

- Overall scatter...
- 10 years of surface pressure data, 2000-2010, NCEP
  - remove mean
  - calculate RMS every 2.5 degrees of latitude and longitude
- largest variability near the poles;
- lowest variability near the equator where there is only small variability in the solar energy over the year

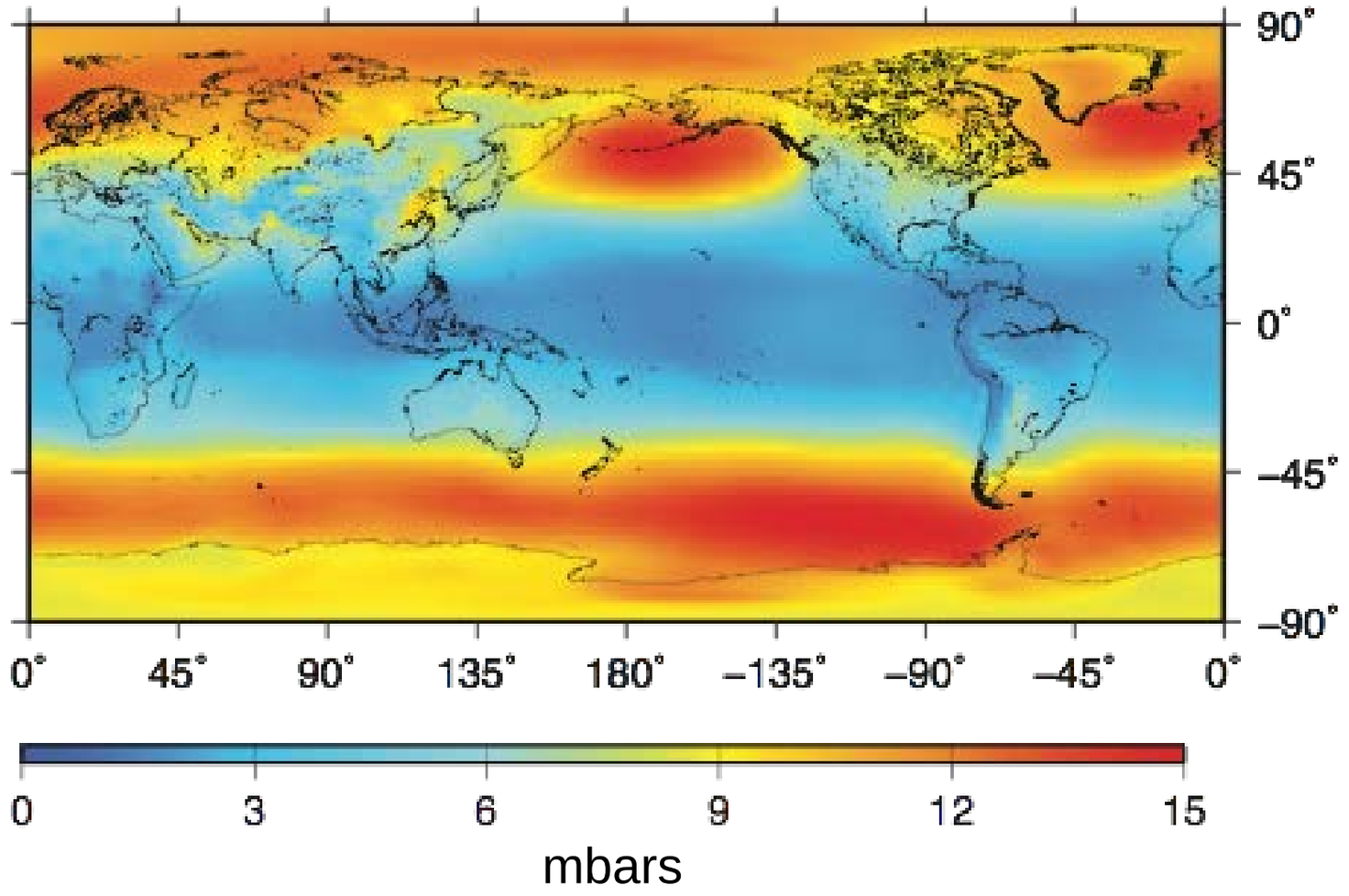

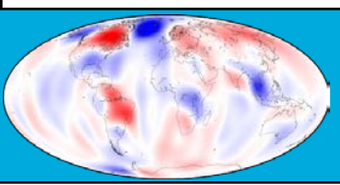

Atmospheric Surface Pressure Data

- National Center for Environmental Prediction (NCEP)
  - Reanalysis
  - Forecast
- European Center for Medium-Range Weather Forecasts (ECMWF)
  - Reanalysis
  - Forecast
- differ in temporal and spatial sampling

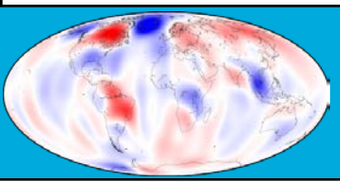

NCEP Grid

- This a plot of the NCEP grid over and near South America
- Pressure is given inside each grid box
  - Some of the grids are entirely over land
  - Some of the grids are over the ocean
  - Some of the grids contain both ocean and land

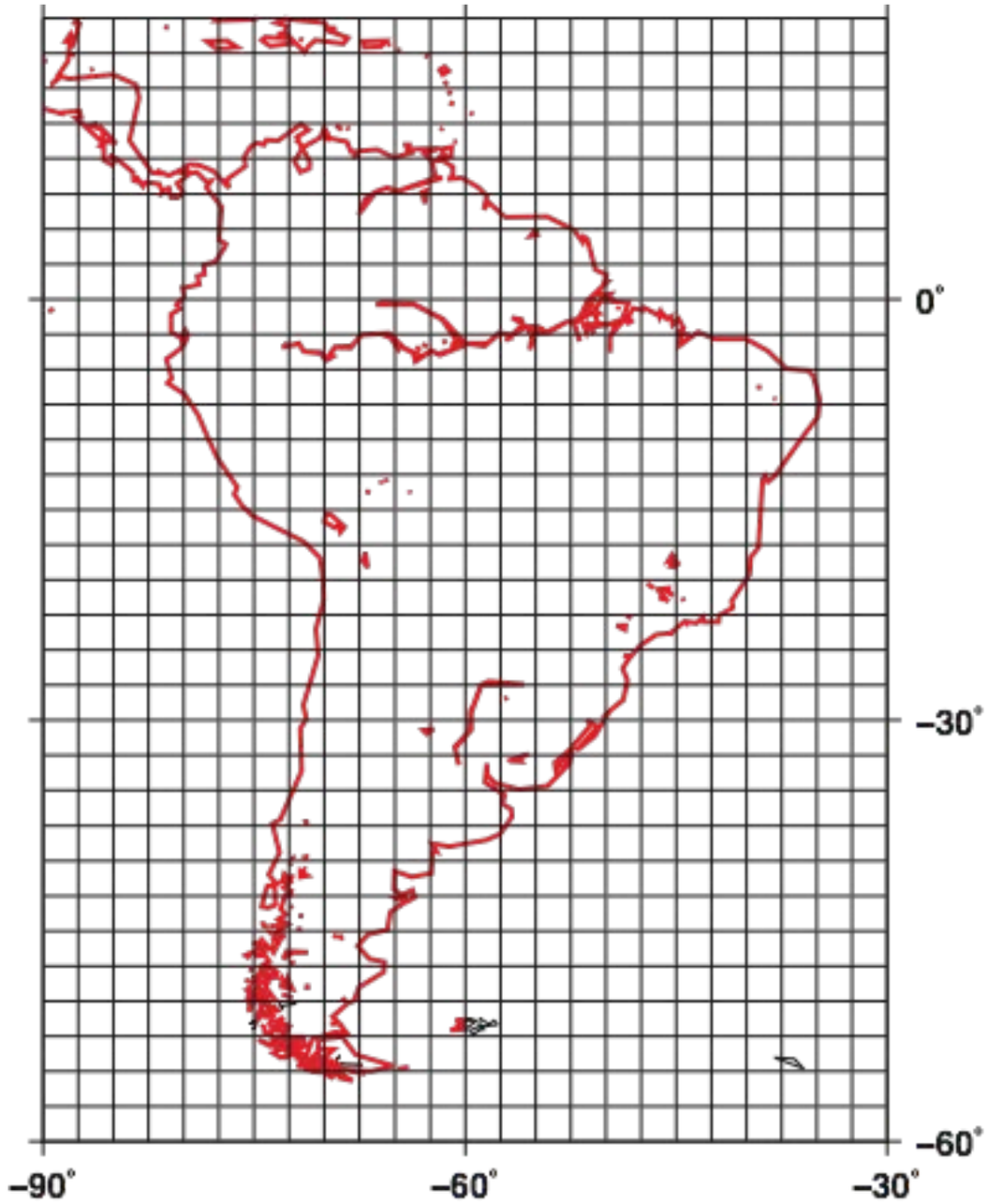

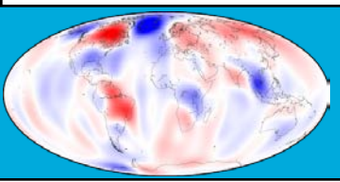

Determining the displacement at a point due to a global grid of pressure

- To determine the displacement at a point due to the pressure change over the entire Earth...

$$dU = \sum_{i=1,144} \sum_{j=1,73} dM_{i,j} G_{i,j}(\Psi) A_{i,j}$$

more or less, the normalizations and conversions to cgs are not shown

- The NCEP grid that I use has a spacing of 2.5º x 2.5º => or 144 data points in longitude and 73 data points in latitude
- $dM_{i,j}$ is the pressure at these data points converted to mass
- $G_{i,j}(\Psi)$ is the Green's function defined at the angular distance between the point where you want to know the displacement and the load...you have a different Green's function for each point where you have pressure

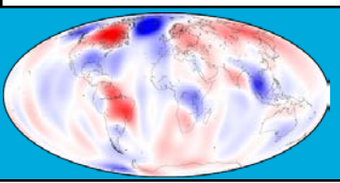

- $A_{i,j}$ is the area of the grid point where the pressure is given
  - Despite the grid being uniform, the grid areas get smaller as you move from the equator toward the poles
- Some of the grid units are over the ocean
- so the equation becomes

$$dU = \left[\sum\sum dM_{i,j} G_{i,j}(\Psi) A_{i,j}\right]_{\text{Land}} + \left[\sum\sum dM_{i,j} G_{i,j}(\Psi) A_{i,j}\right]_{\text{Ocean}}$$

- and each sum is only over the grid points where there is land OR ocean

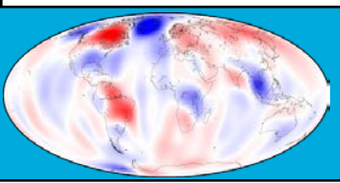

- But how do the oceans respond to changes in atmospheric pressure?
- If you look at one place in the ocean, and you look at surface pressure changes with a frequency longer than a day, you will notice that when the pressure increases the water moves out of the way so that the total load acting on the ocean floor is unchanged
- This is known as the inverted barometer (IB) effect

$$P_1 = (\rho_{\mathrm{Air}} \times h_{\mathrm{Air}} + \rho_{\mathrm{H2O}} \times h_{\mathrm{H2O}}) \times \textit{Area of Column}$$

$$P_2 = (\rho_{\mathrm{Air}} \times h_{\mathrm{Air}} + \rho_{\mathrm{H2O}} \times h_{\mathrm{H2O}}) \times \textit{Area of Column}$$

$$\textit{Area of Column} = d \times w$$

if IB, then $P_1 = P_2$

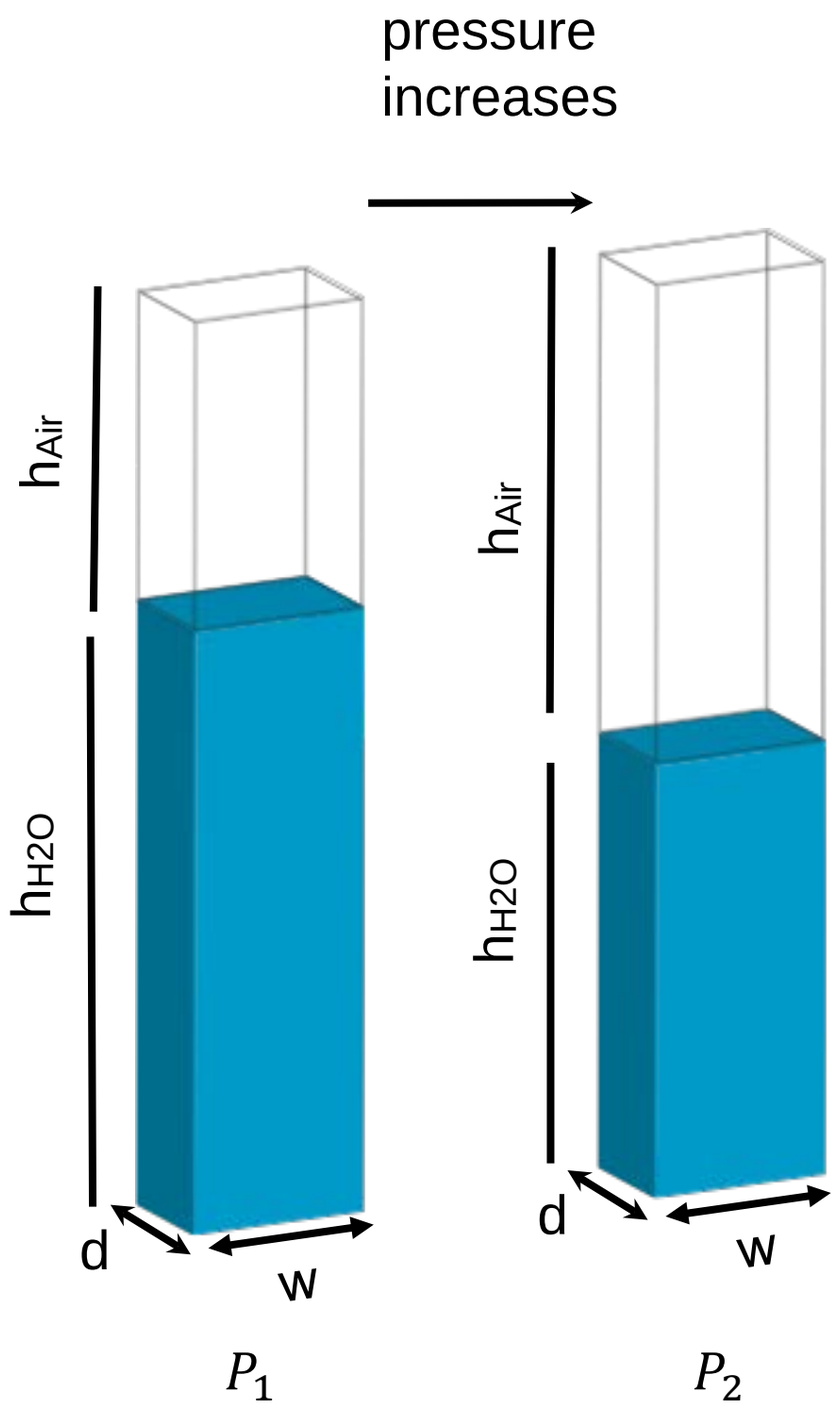

- The inverted barometer is theoretically true IF the total mass of the air over the oceans doesn't change
- If this net mass does change, then we have a constant force acting over the entire ocean floor

$$\rho_0 = \frac{\sum_{i,j} p_{i,j} A_{i,j}}{\sum_{i,j} A_{i,j}}$$

Sometimes referred to as the modified IB in the literature

- $A_{i,j}$ is the area of the ocean grid unit
- $p_{i,j}$ is the pressure change over that ocean grid unit
- The sum is over all grid units that are over the ocean
- ρ_0 replaces $dM_{i,j}$ in the summation over the ocean (the right hand side of the equation)

$$dU = \left[\sum\sum dM_{i,j} G_{i,j}(\Psi) A_{i,j}\right]_{\text{Land}} + \left[\sum\sum \rho_0 G_{i,j}(\Psi) A_{i,j}\right]_{\text{Ocean}}$$

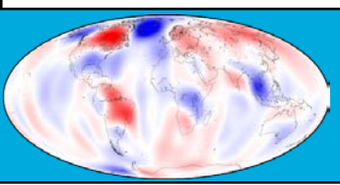

Radial displacements due to atmospheric pressure loading

- NCEP reanalysis
  - global
  - 6 hourly
  - 2.5^{o} x 2.5^{o}
  - comes as netcdf format
- Modified IB ocean response determined from the 2.5 degree land/ocean mask
- Mixed land/ocean grids?

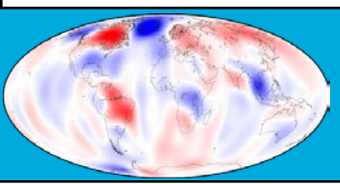

- Sometimes a single grid 2.5 x 2.5 degree grid unit, contains both land and water, such as that shown to the right. What do I do in this case?
- The orange represents land.
- For these mixed grids, they are subdivided into 0.25 x 0.25 degree grid cells
- Then I use ETOPO5 at the 0.25 degree resolution to make a land-ocean mask
- The new mask looks like the bottom figure

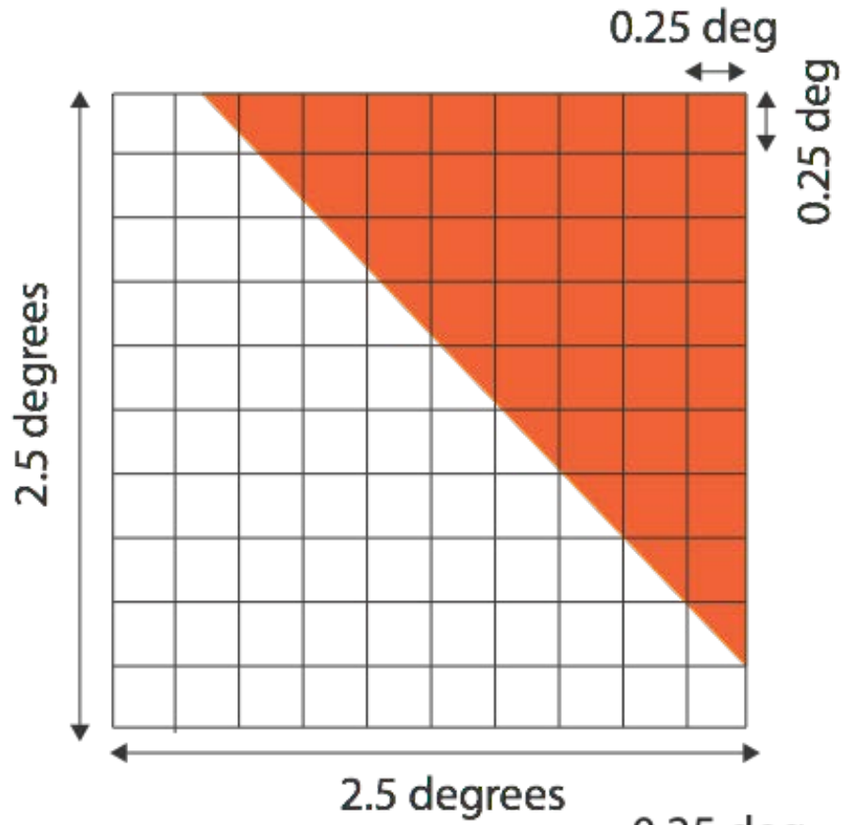

- Based on this refined mask, I determine the land area and the ocean area of the 2.5 degree grid unit
  - For the 0.25 deg land cells, I determine the separate Green's Functions and sum them up
  - For the 0.25 ocean cells, I similarly determine the separate Green's Functions and sum them up
  - Now the 2.5 degree land/ocean grid unit has a GF_{land} and a GF_{ocean}
  - The GF_{land} is put into the sum and multiplied by the load of the original 2.5 degree grid unit
  - The GF_{ocean} is also put into the sum and multiplied by the load defined by the Modified IB
  - The error introduced into the calculation by using the 2.5 degree land/ocean mask instead of the 0.25 mask is very small
- Now that all the preliminaries have been taken care of, let's look at the radial displacement at a particular location...

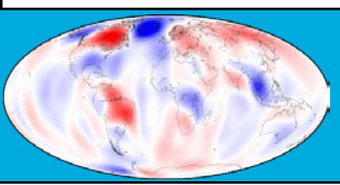

- POTS

Potsdam, Germany

- displacement is inversely proportional to the load

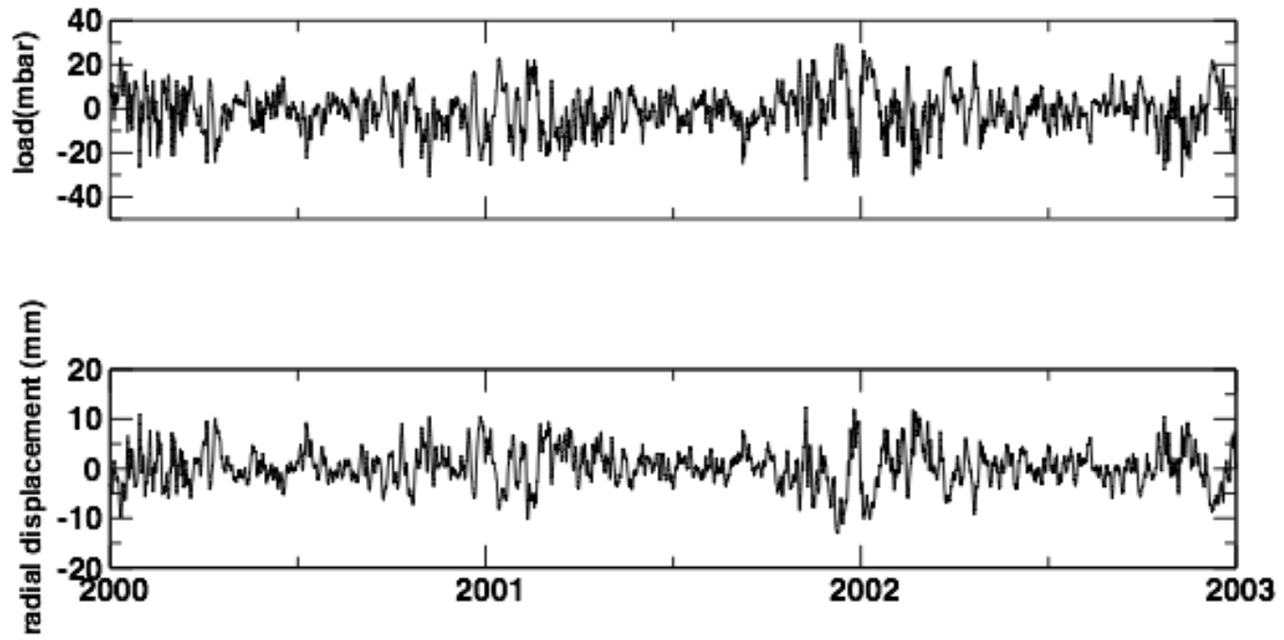

Admittance is not constant over all days; it depends on the size of the pressure cell.

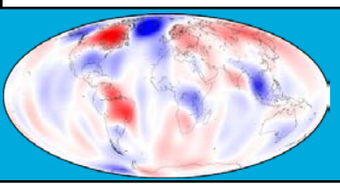

Horizontal displacements due to atmospheric pressure loading

- note the scale difference between the up and the horizontal components
- for POTS, the RMS of the up or radial is 6 times that of the horizontal
- Annual signal can be observed
  - Largest displacements in the winter
  - Smallest in the summer

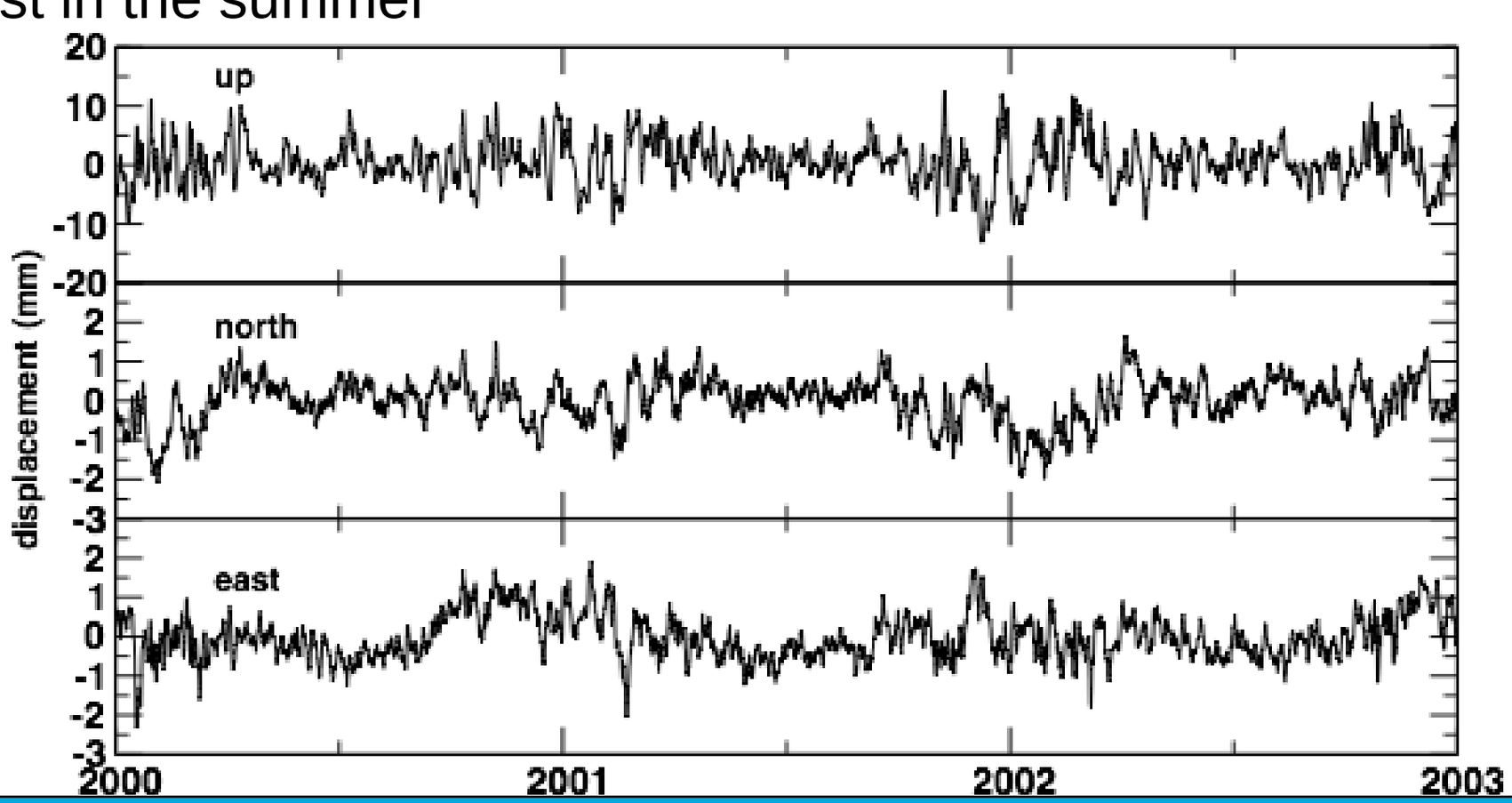

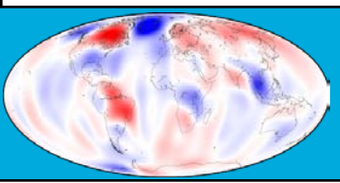

What about globally?

- RMS of the radial surface displacement
- RMS of the horizontal surface displacement; NOTE the difference in scale between the radial and the horizontal, a factor of 5
  - horizontal = $\sqrt{dN^2 + dE^2}$
- Globally the scatter on the horizontal is a factor of 5 smaller than the vertical
- Larger variability at mid- to high-latitudes
- Coastal areas less affected by loading due to the ocean response that tends to mitigate the effects of loading

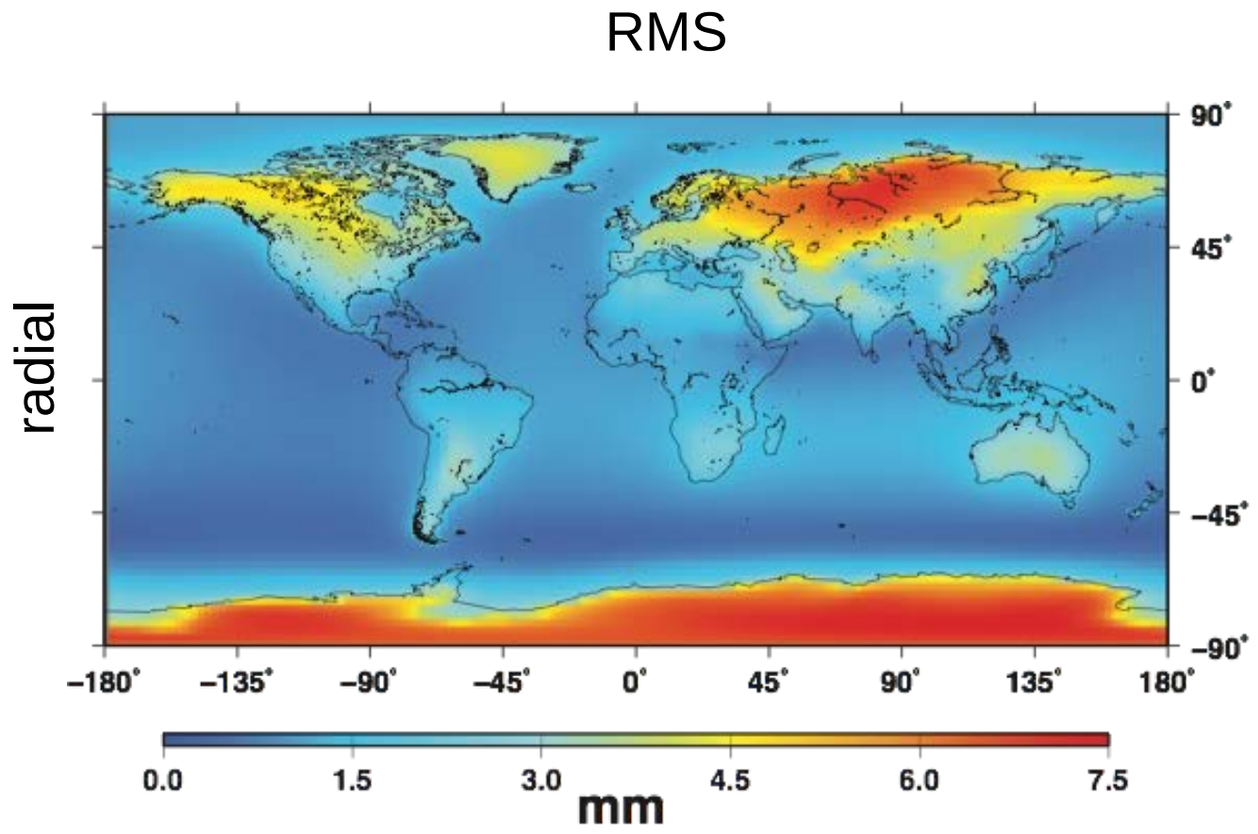

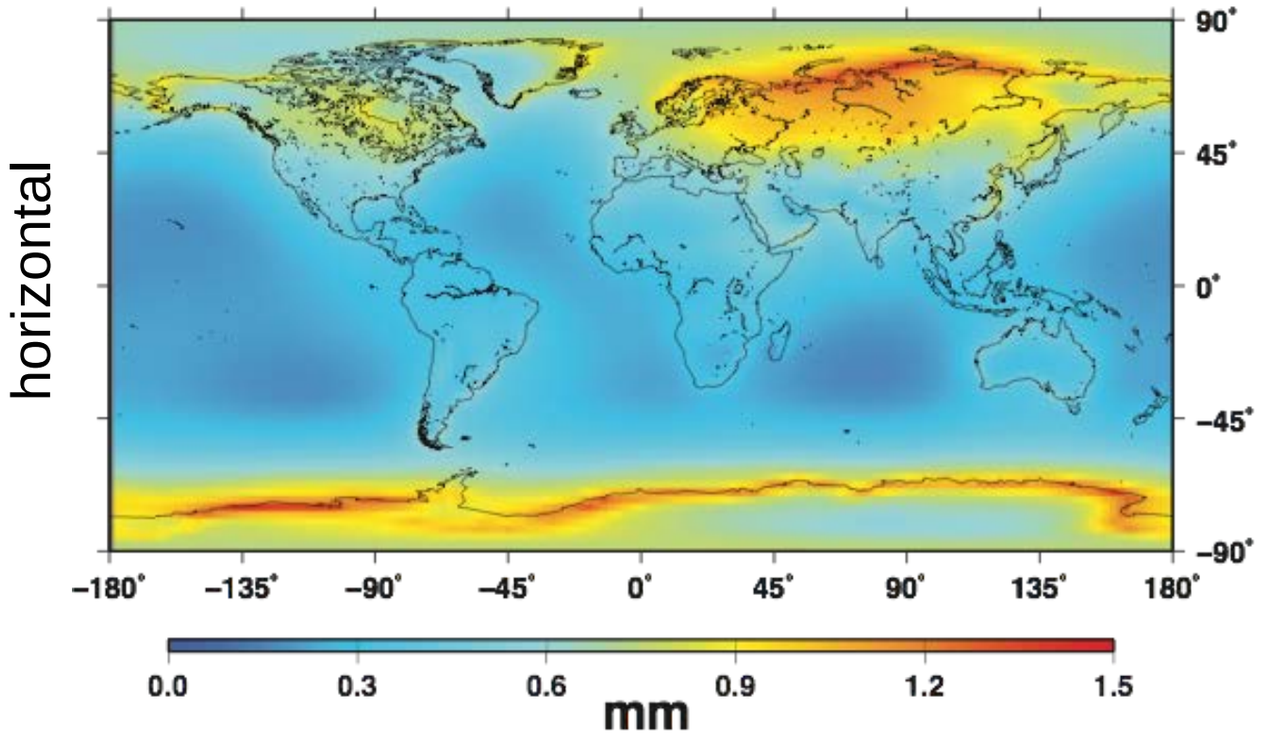

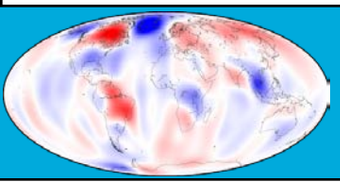

Some details of the loading calculation...

- I did not use the surface pressure as output from the NCEP file
  - I removed a 30 year mean as I am only interested in relative surface displacements not absolute displacements
- You must choose a reference frame for your displacements
  - The Green's Functions in Farrell, 1972 are given in the Center of Earth Frame (CE)

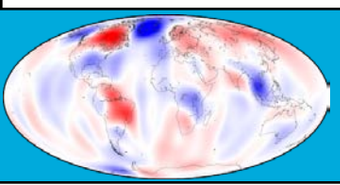

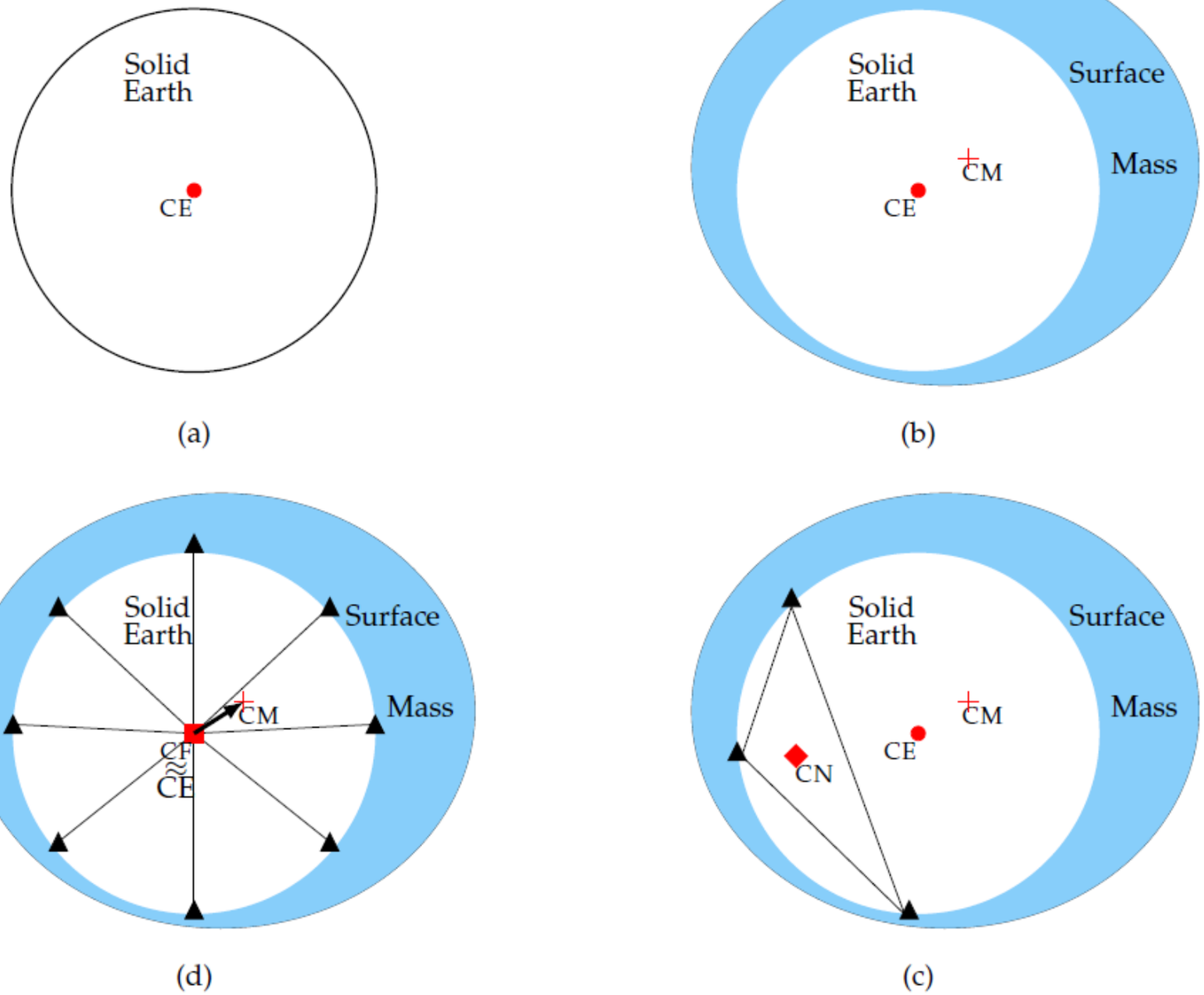

- The clockwise sketches illustrate the different geodetic reference frames used in satellite geodesy. Subfigure (a) shows the Center of the solid Earth (CE) and subfigure (b) illustrates the Center of the Earth system (CM), which includes the solid Earth and its surface mass. Subfigure (c) and (d) display the Center of Network (CN) and the Center of Figure (CF), respectively. In essence, CF is the one extreme example of CN with a globally and uniformly distributed tracking stations. Subfigure (d) also presents the vector pointing from the origin of CF to the origin of CM and the time evolution of this vector is called geocenter motion.

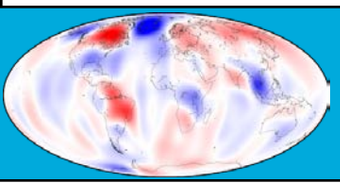

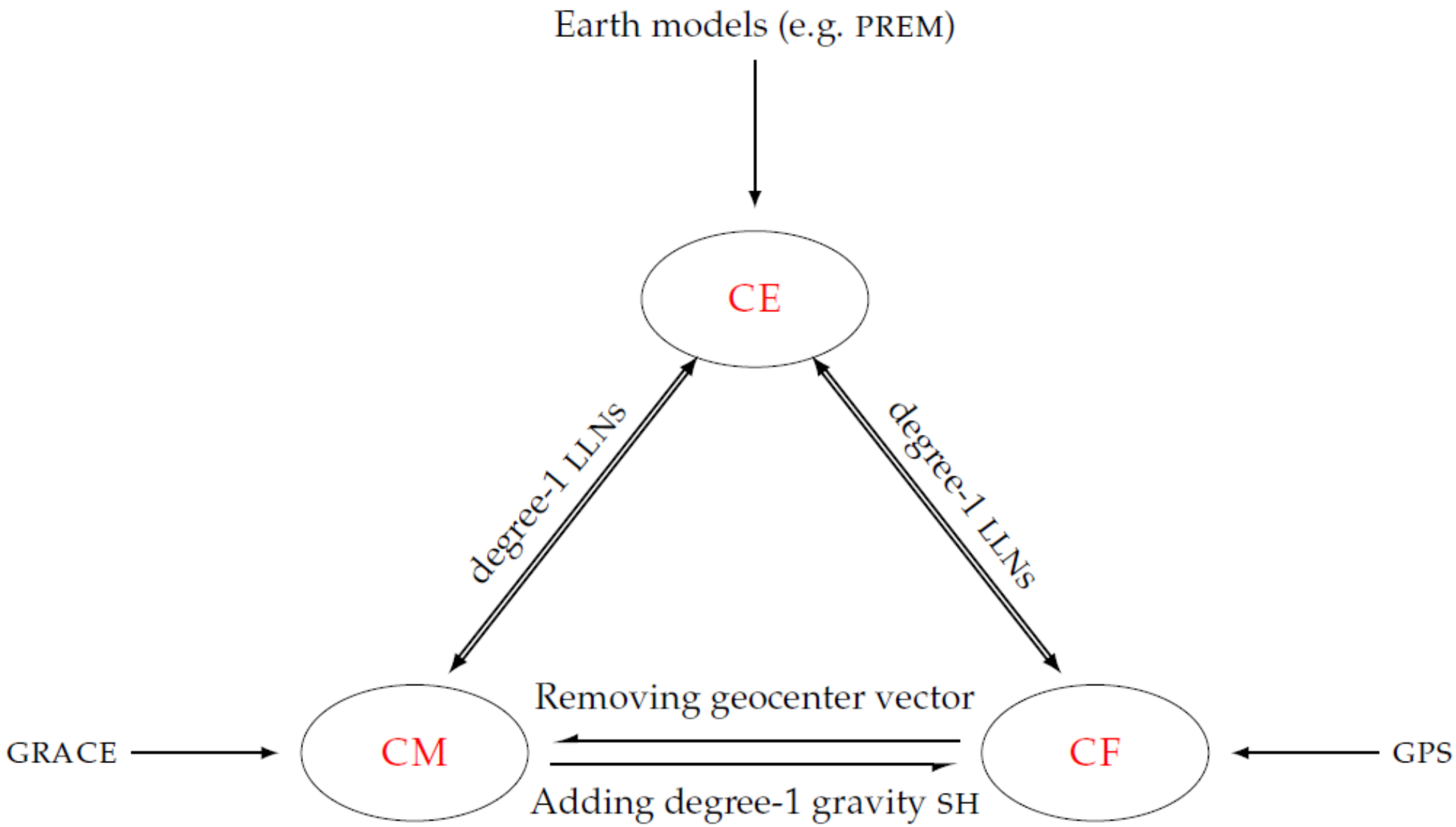

- Mutual relationships between CE, CM and CF, with connection to the Earth models, the GRACE and GPS datasets, respectively.

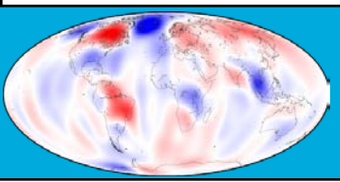

How good are the models?

- Let’s compare atmospheric loading (ATML) with GPS data
- From this slide onward, we observe the greatest scatter in the up and horizontal in Siberia
- To look for GPS stations in the region, you can start by looking at the site http://igscb.jpl.nasa.gov/network/netindex.html
- The IGS (International GNSS Service) provides information on GPS/GNSS stations in the IGS network

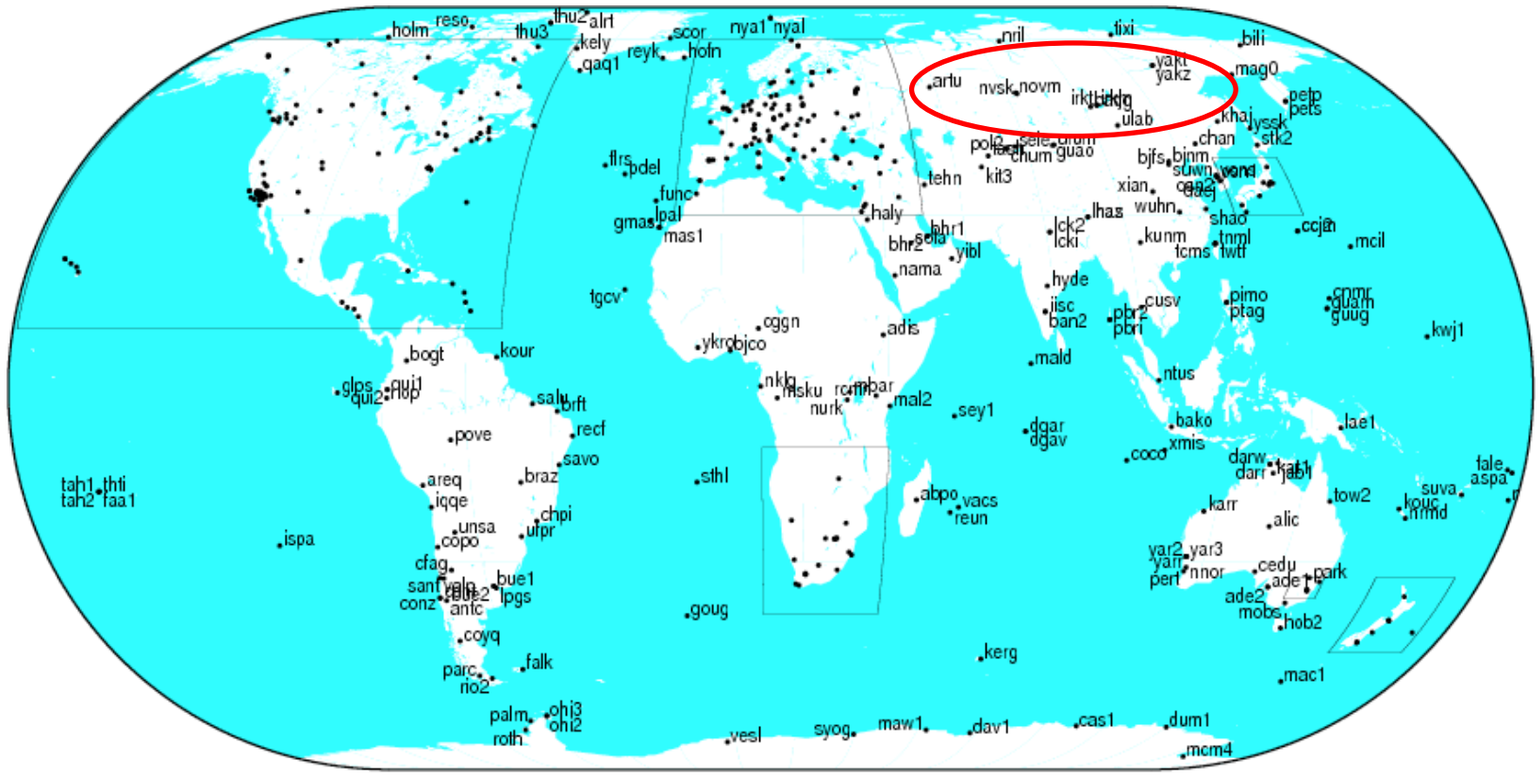

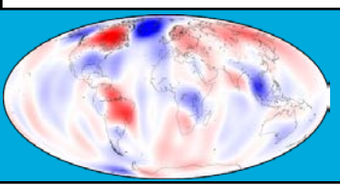

GPS Data

- Weekly SINEX files from MIT solution provided by X. Collilieux, Z. Altamimi, and P. Rebischung IGN (Paris, France)
- Only use time series with more than 100 observations for statistical reasons
- 6-hourly ATML averaged into weekly values centered on the GPS week

Station	Location	Longitude	Latitude
artu	Arti Russian Federation	58.57	56.43
irkt	Irkutsk, Russia	104.32	52.22
nvsk	Novosibirsk, Russia	83.24	54.84
yakt	Yakutsk, Russian Federation	129.68	62.02

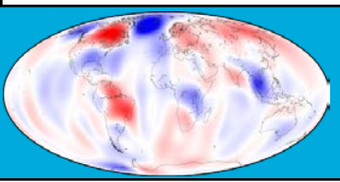

- Peak-to-peak radial surface displacements of 60 mm!
- Strong annual signal
- Model does a good job of removing the signal
- In all cases, model reduces the signal in the data

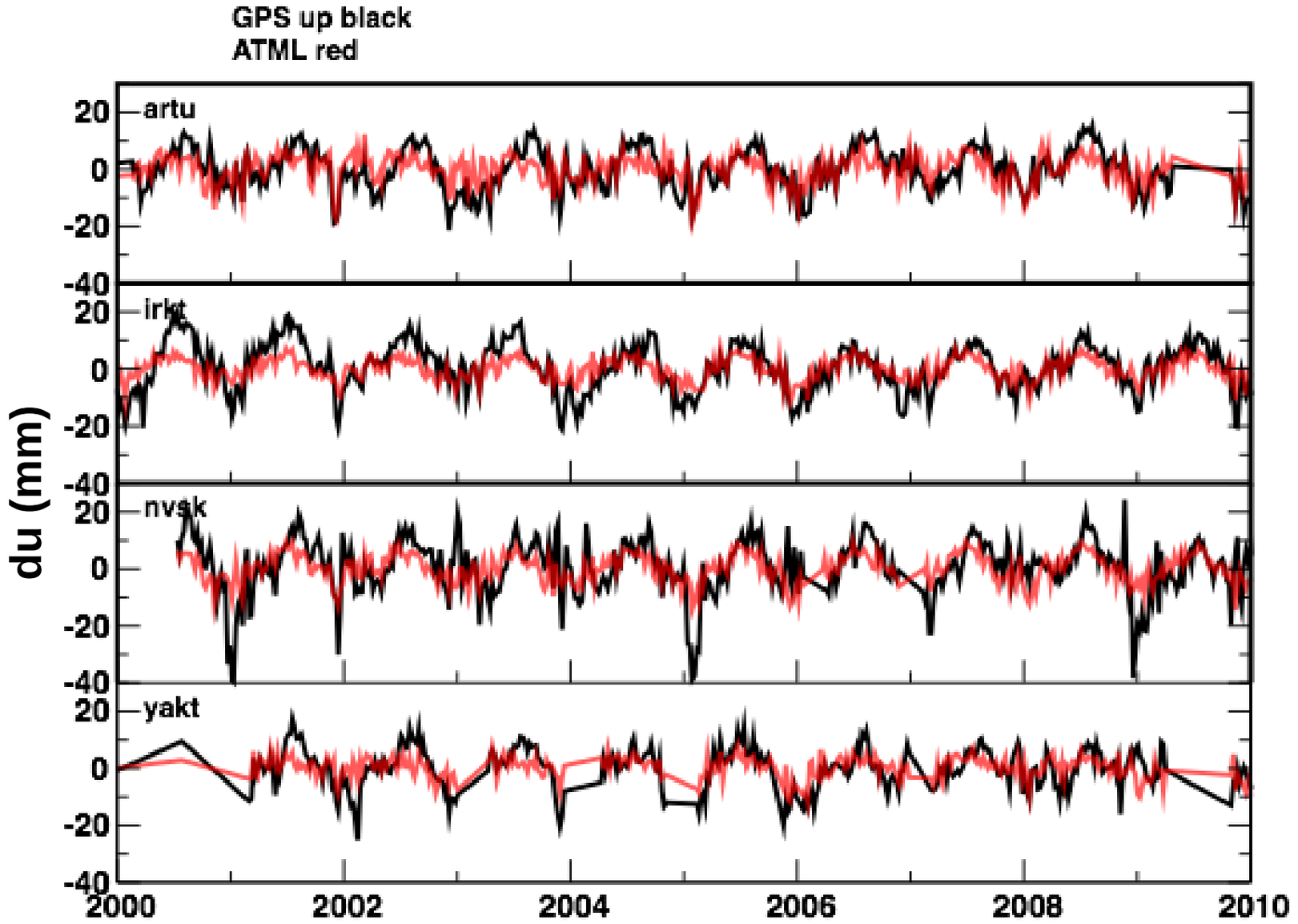

- Define the percent change in RMS as

$$\%\Delta\mathrm{WRMS} = \frac{\mathrm{WRMS}_{\mathrm{GPS}} - \mathrm{WRMS}_{\mathrm{GPS-ATML}}}{\mathrm{WRMS}_{\mathrm{GPS}}}$$

Station	WRMS(GPS) (mm)	WRMS(ATML) (mm)	WRMS(GPS-ATML) (mm)	%ΔWRMS
artu	7.2	4.7	5.4	25
irkt	8	3.7	5.5	31.3
nvsk	9.8	5	8	18.4
yakt	6.8	3.7	5.6	17.6

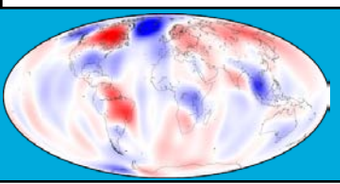

Globally?

- Top panel is the WRMS of the GPS up coordinate alone; bottom is the GPS up corrected for the ATML
- Siberia, Australia, sites in Europe, Canada and South America have the RMS removed when ATML is removed
- Still difficult to see globally the effect.
- 499 stations out of 690 have the WRMS of the up coordinate reduced when corrected for ATML

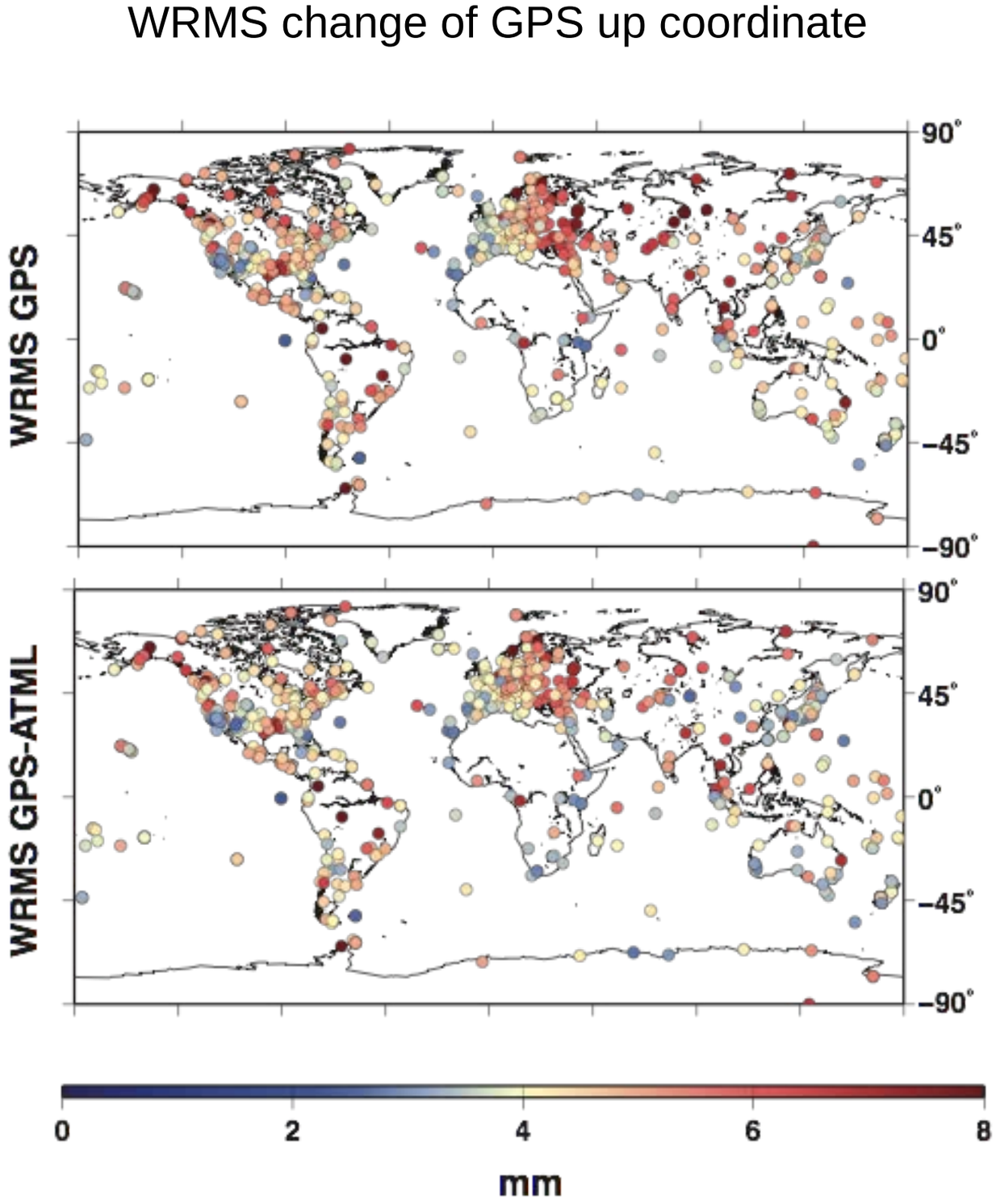

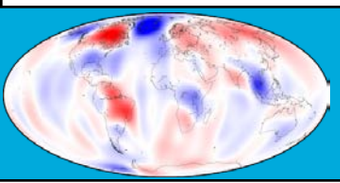

Global %ΔWRMS GPS up

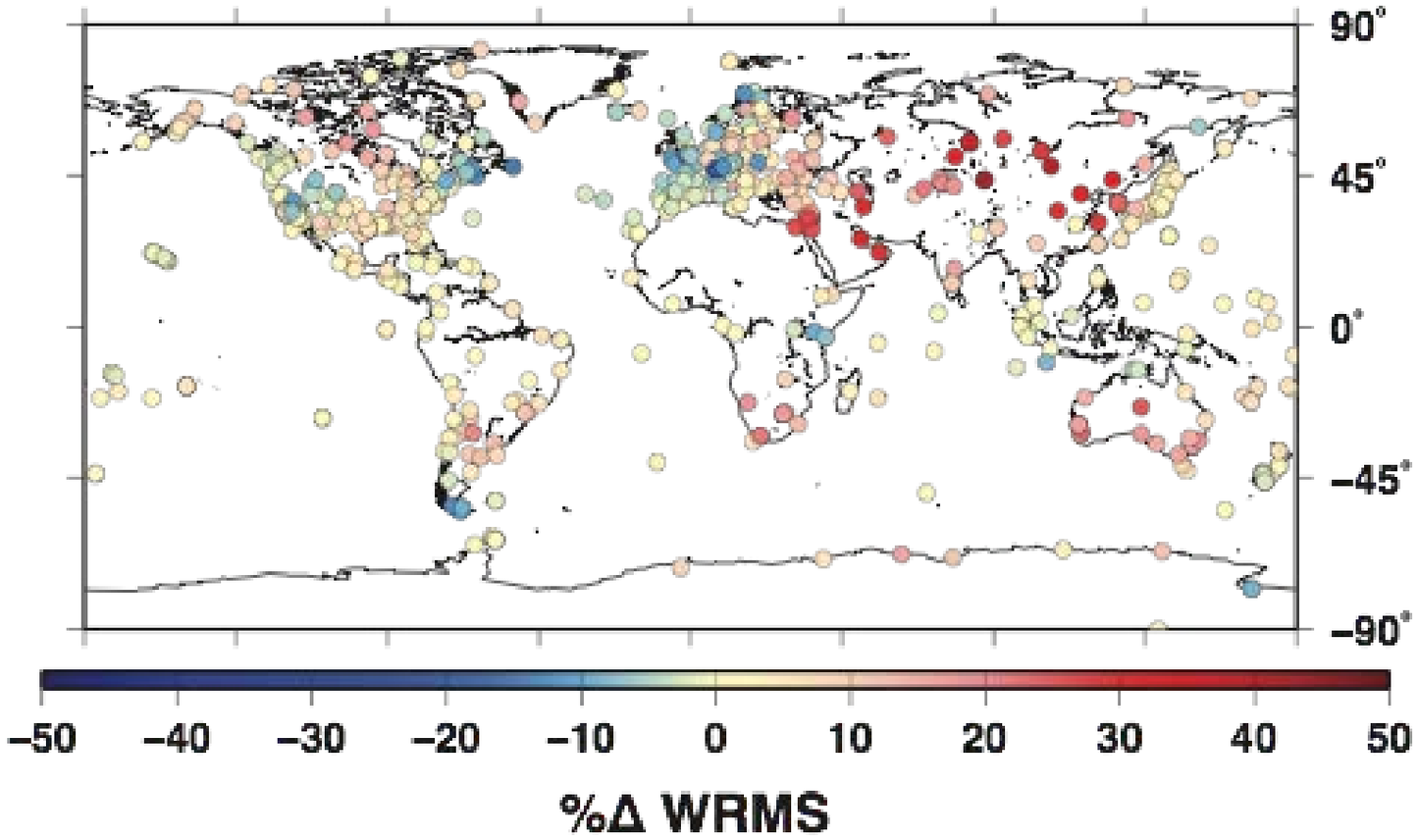

- Pink to red: stations where the WRMS of the GPS up is reduced when ATML correction is applied
- Blue to yellow: stations where the WMRS of the GPS up is increased => ATML signal adds noise to the GPS time series
- Asia, Australia, and Northern North America show significant %ΔWRMS
- ATML signal not significant at many coastal and island sites due to the IB response of the oceans

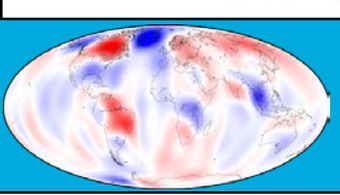

What about the horizontals?

- Of the 690 GPS time series analyzed the ATML model can reduce the WRMS on
  - 358 or 52% in the North
  - 422 or 61% in the East
  - 499 or 72% in the Up
- The average WRMS reduction is
  - 0.1% in the North
  - 1% in the East
  - 4.5% in the Up

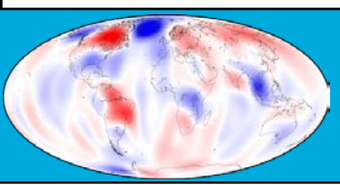

4. Continental Water Storage Loading

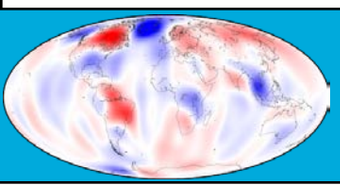

The Hydrological Cycle

- The hydrological cycle represents the continuous movement of water on, above, or below the surface of the Earth
- Water can exist in all physical states: liquid, gas, or solid
- The total amount of water on the Earth is fairly constant
  - But the amount of water in any reservoir varies with time
  - Water cycles between the atmosphere, the ocean, the cryosphere, continental water (rivers, lakes, groundwater, soil moisture, etc.)
  - Transport between the reservoirs is driven by the physical processes of evaporation, condensation, precipitation, infiltration, runoff, and subsurface flow

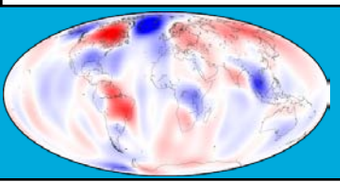

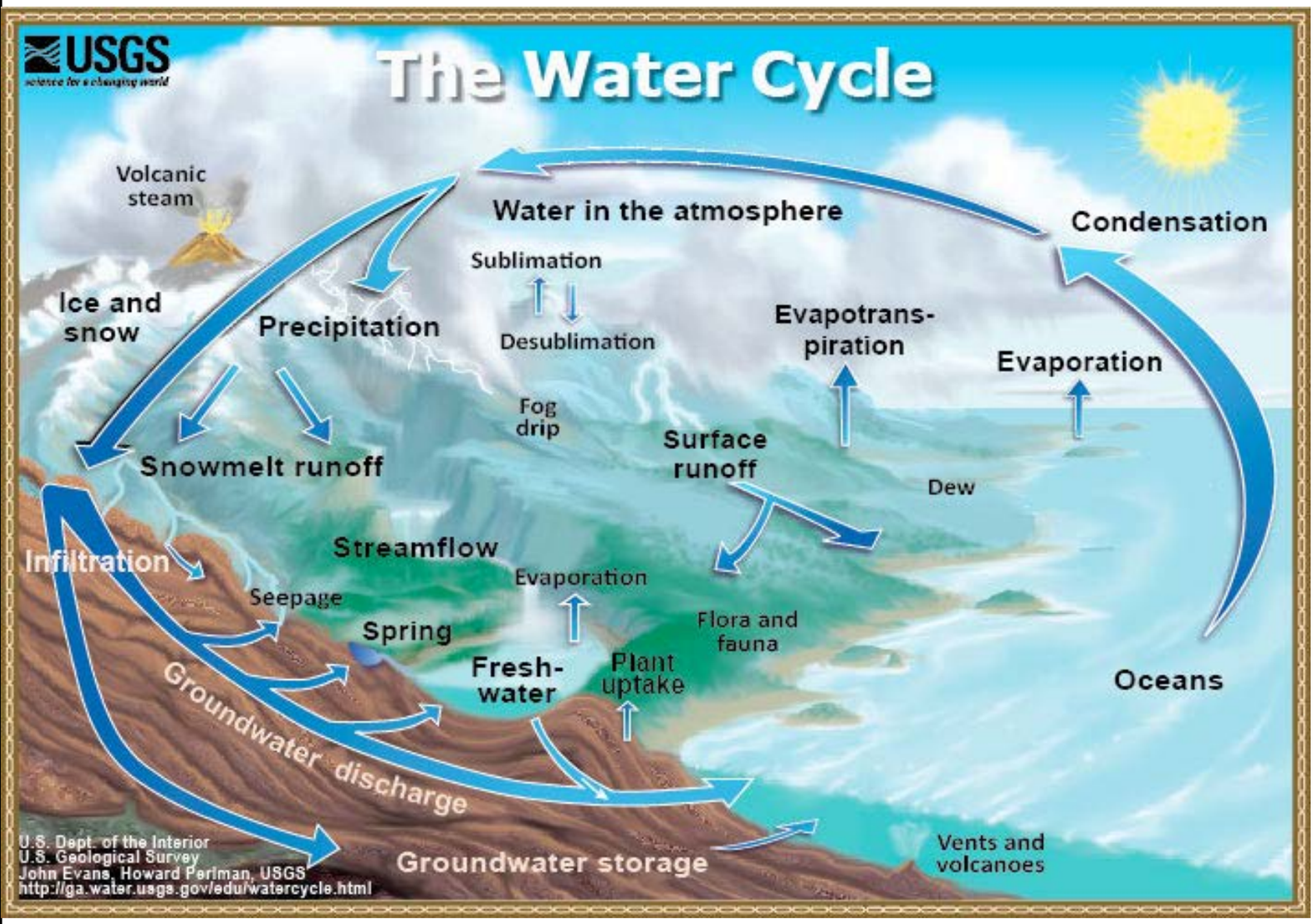

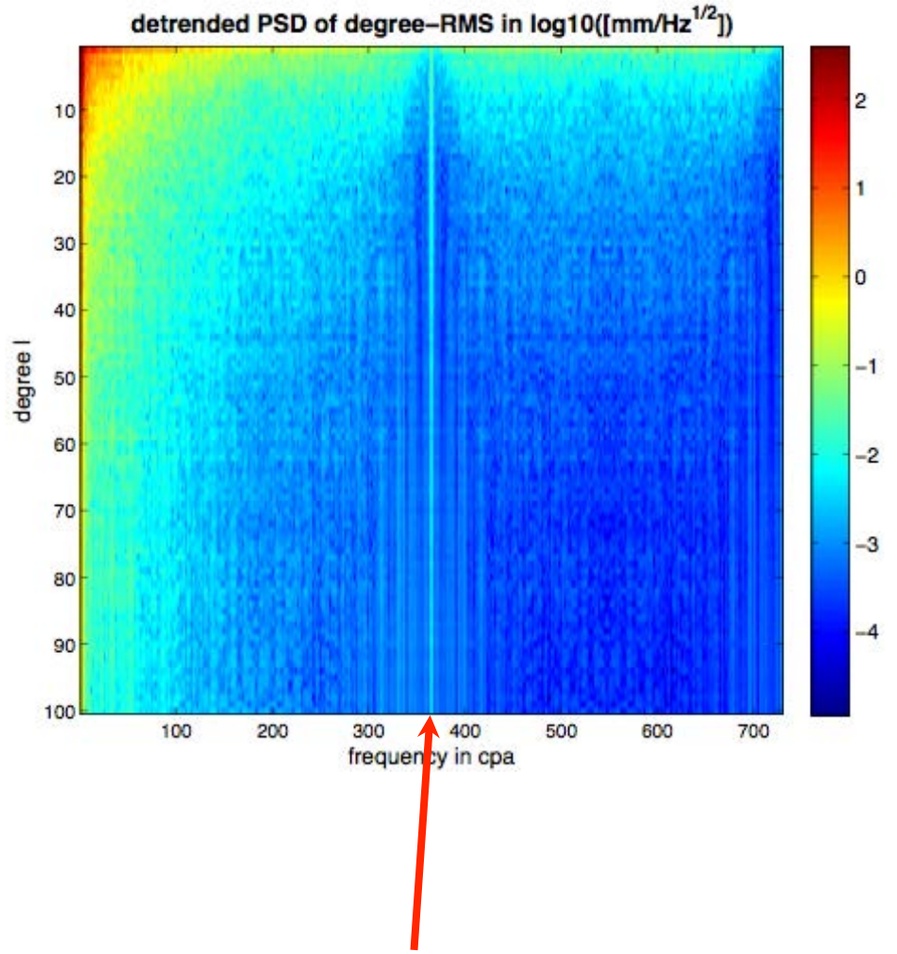

http://ga.water.usgs.gov/edu/watercyclesummary.html

- Hydrological cycle is driven by Energy from the Sun
- Energy from the Sun varies as a function of time of the year
- Strongest period in the hydrological cycle will be annual

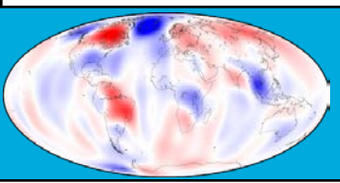

Continental water-storage loading models

Model	Data source	Unit	Temporal resolution	Spatial resolution (degree)	Latency
GLDAS-A (NOAH)	SM (4 layers)	kg/m^2	Monthly	1×1	1–4 months
	SWE	kg/m^2			
NCEP-R-2	SM (2 layers)	m^3/m^3	6-hourly	$1.875 \times (1.8889 - 1.9048)$	3–4 days
	SWE	kg/m^2			
GLDAS-B (NOAH)	SM (4 layers)	kg/m^2	3-hourly	1×1	1–4 months
	SWE	kg/m^2			
MERRA-A	PRMC	m^3/m^3	Monthly	$2/3 \times 1/2$	1–2 months
	SNOMAS	kg/m^2			
MERRA-B	PRMC	m^3/m^3	1-hourly	$2/3 \times 1/2$	1–2 months
	SNOMAS	kg/m^2			

- Except above models, we also have WGHM (WaterGAP Global Hydrological Model) and LSDM (Land Surface Discharge Model) from GFZ.

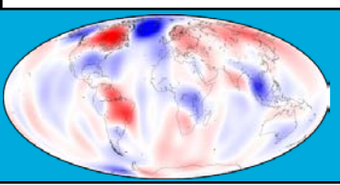

GLDAS

- A high-resolution estimates of terrestrial water and energy storages that can be used to predict climate change, weather, flooding, etc.
- Stores of energy and water fluctuate between land and the atmosphere at diurnal, seasonal, and inter-annual time scales
- GLDAS uses ground and space-based observation systems that provide the data to constrain modelled land surface states
- GLDAS-NOAH
  - Monthly resolution
  - 1º x 1º spatial resolution
  - Dynamics for snow is poorly modeled so remove Greenland and Antarctica from the input model

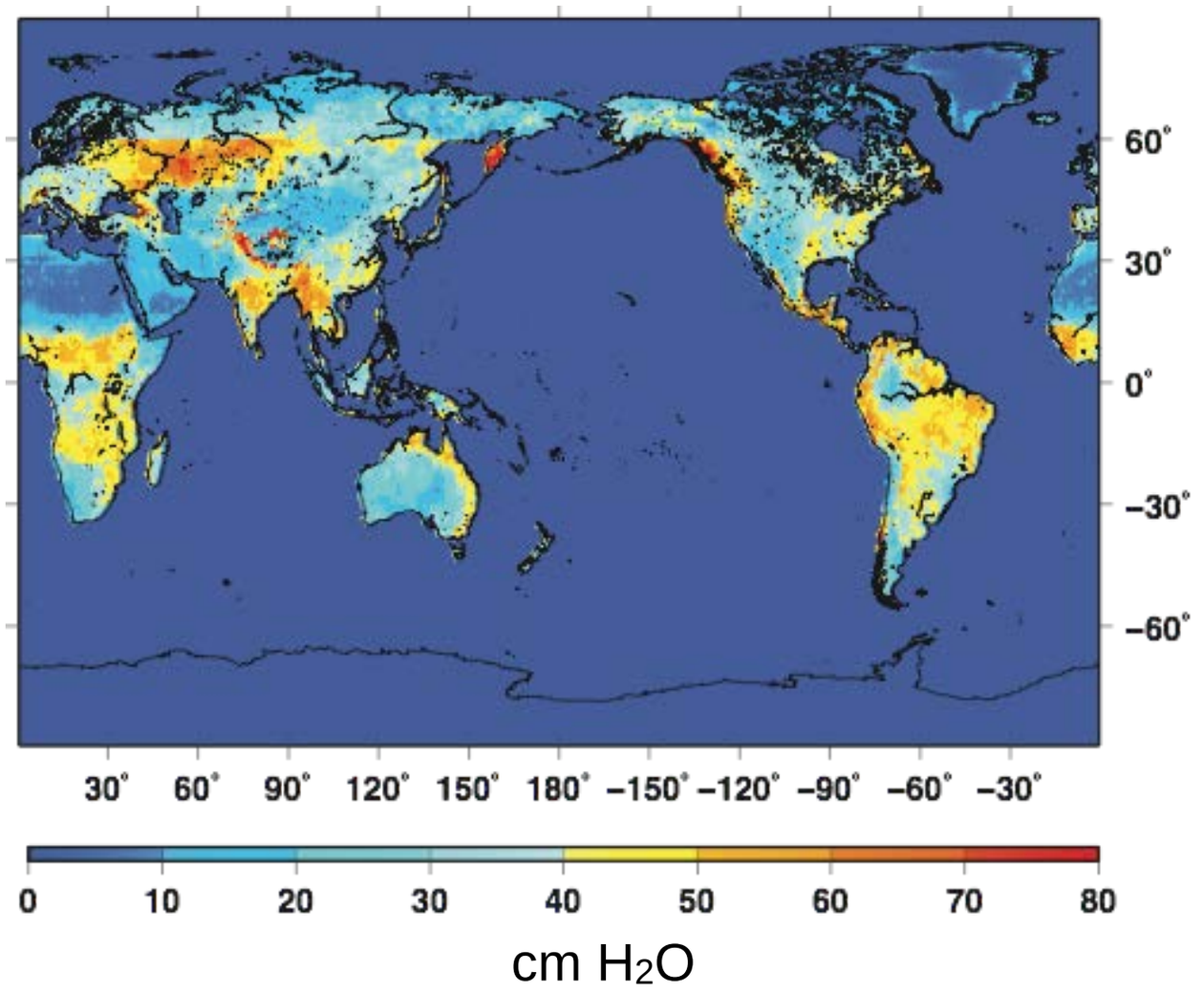

Image shows the maximum range in water storage from 01-1979 to 12-2011

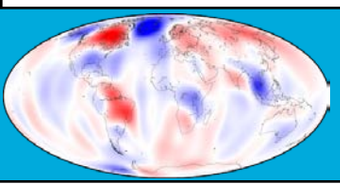

- GLDAS Annual hydrology: from *Tapley, B.D.* et al., 2004.

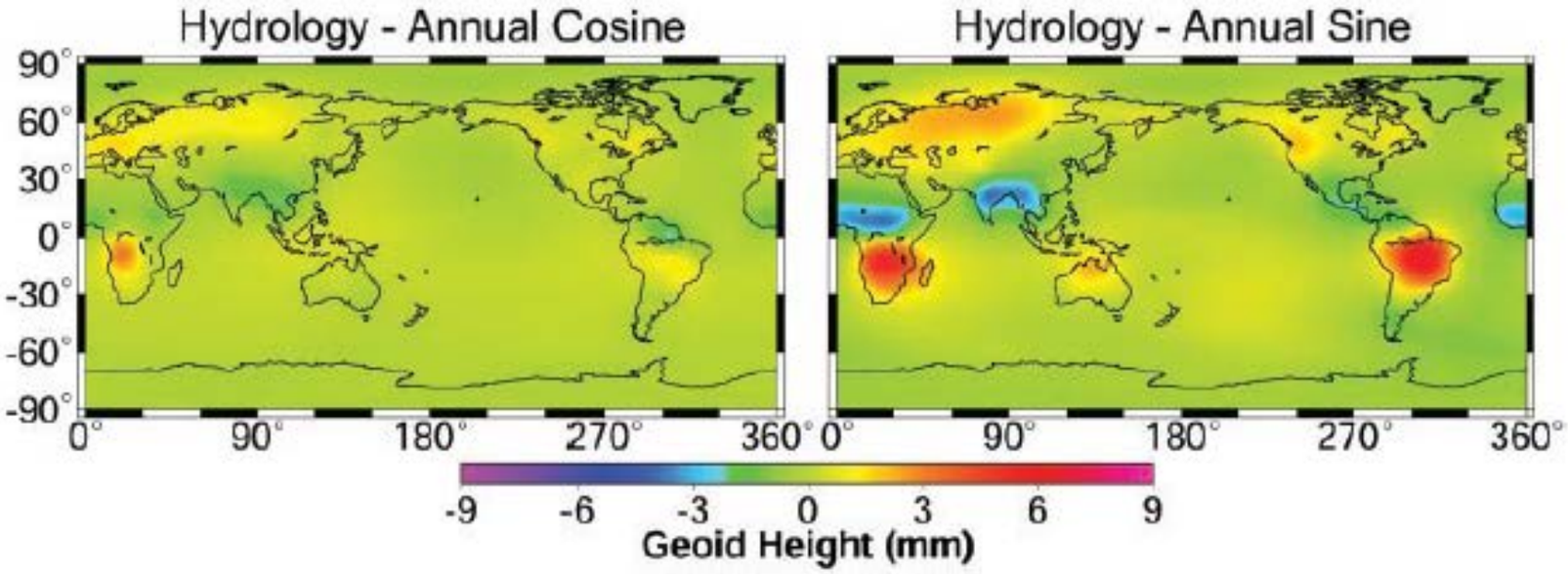

- Large annual changes over the Himalaya, Amazon, and the Intertropical Convergence Zone (ITCZ) over Africa

Intertropical Convergence Zone

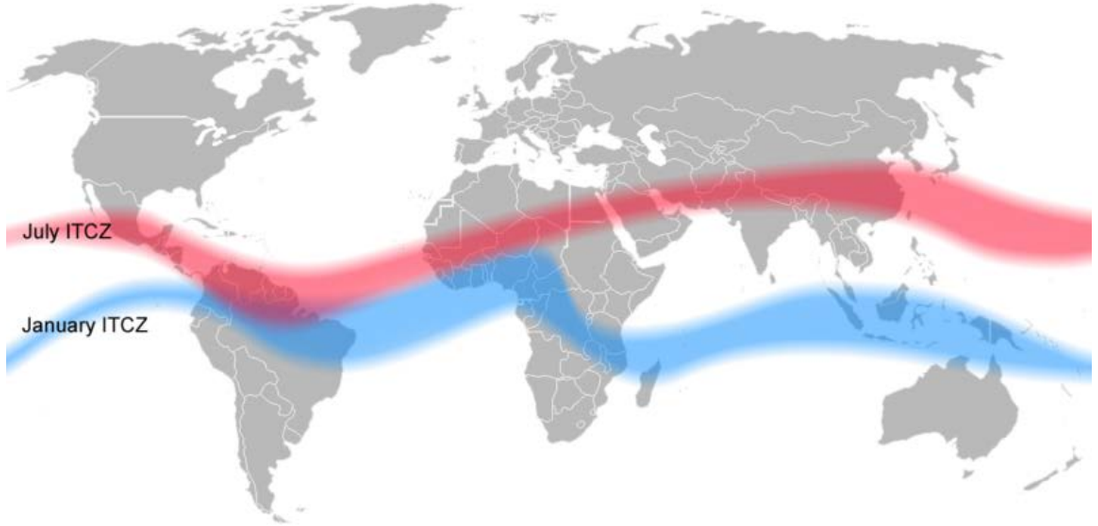

http://en.wikipedia.org/wiki/Intertropical_Convergence_Zone

Tapley, B.D., Bettadpur, S., Ries, J.C., Thompson, P.F., Watkins, M.M., 2004, GRACE measurements of mass variability in the Earth system, Science (New York, N.Y.), 305, 503–505. ext

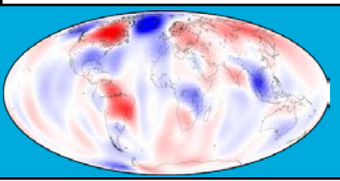

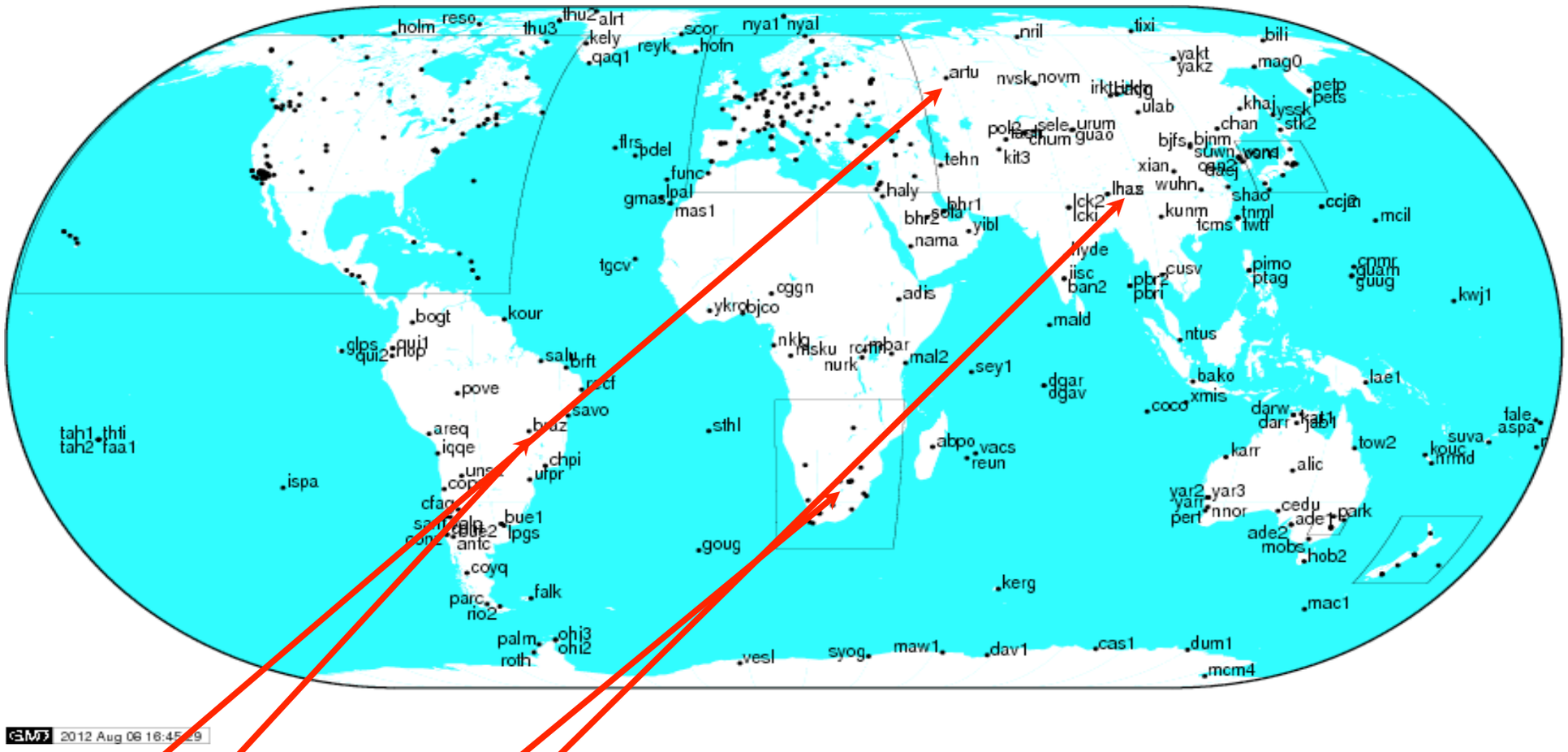

GMT 2012 Aug 08 16:45:29

Station	Location	Longitude	Latitude
artu	Arti, Russian Federation (Siberia)	58.56	56.43
braz	Brasilia, Brazil (Amazon)	312.12	-15.94
hrao	Krugersdorp, South African (ITCZ)	27.69	-25.89
lhas	Lhasa, China (Himalaya)	91.1	29.66

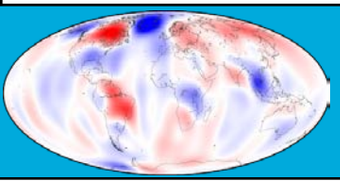

- GPS up coordinate versus the GLDAS up
- Strong annual signal

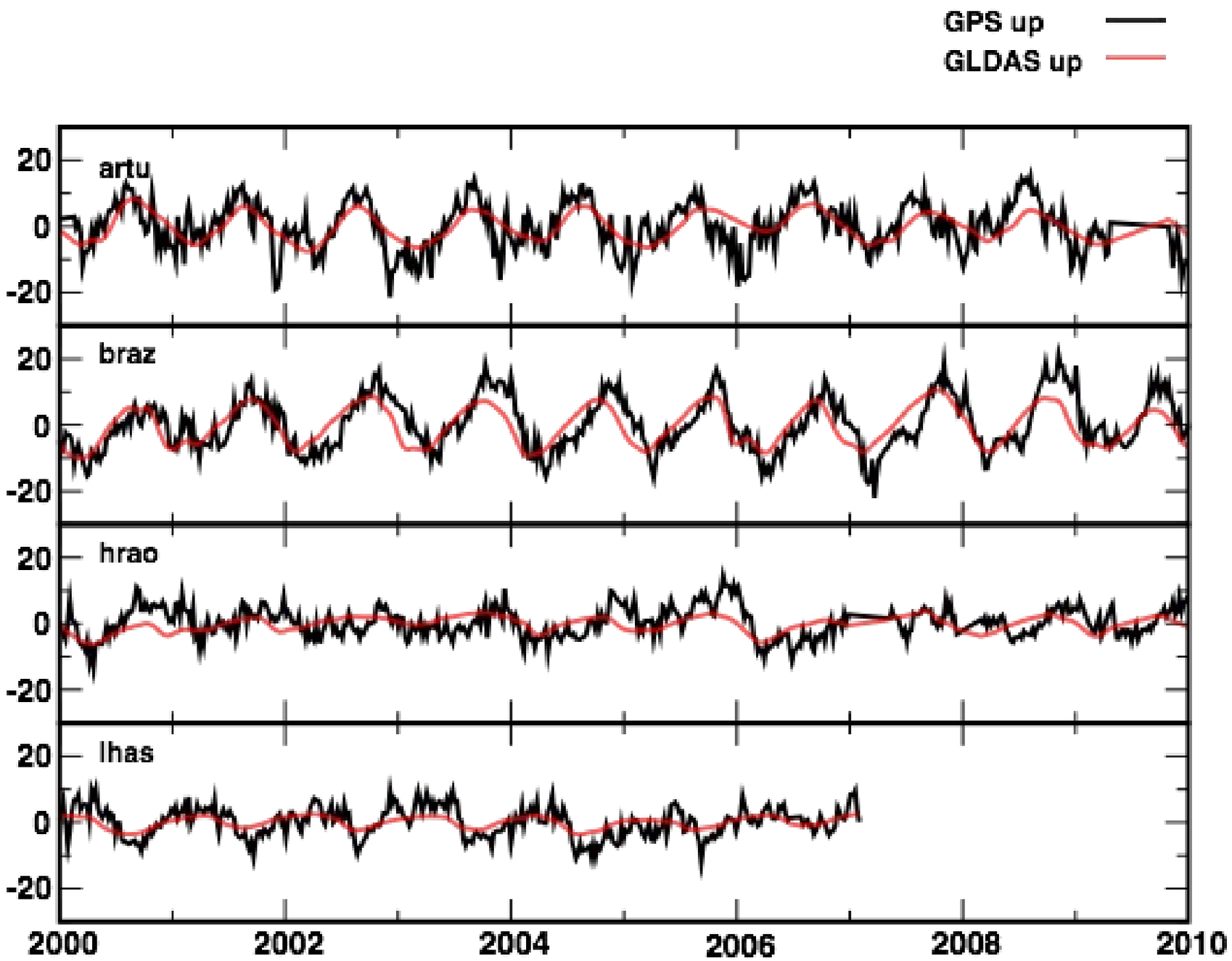

Station	WRMS(GPS) (mm)	WRMS(GLDAS) (mm)	WRMS(GPS-GLDAS) (mm)	%ΔWRMS
artu	7.2	4.1	5.5	23.6
braz	7.6	5.6	5.1	32.9
hrao	12.4	2.2	12.5	-0.8
lhas	4.3	1.9	3.5	18.6

- The model does not improve the WRMS at hrao
- WRMS reduced when GLDAS model is applied
  - North: 498 out of 690 sites (72% of sites have WRMS reduced)
  - East: 431 out of 690 sites (62% of sites have WRMS reduced)
  - Up: 571 out of 690 sites (83% of sites have WRMS reduced)

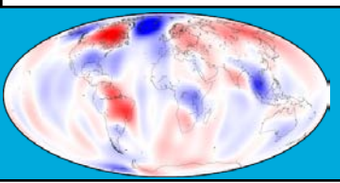

Globally?

- Top panel is the WRMS of the GPS up coordinate alone; bottom is the GPS up corrected for the CWS model
- Looking for dots in the upper panel to turn from red to a lighter color or even yellow or blue in the bottom panel
- Europe, Eastern Europe, North America, and South America GLDAS does well at removing the signal

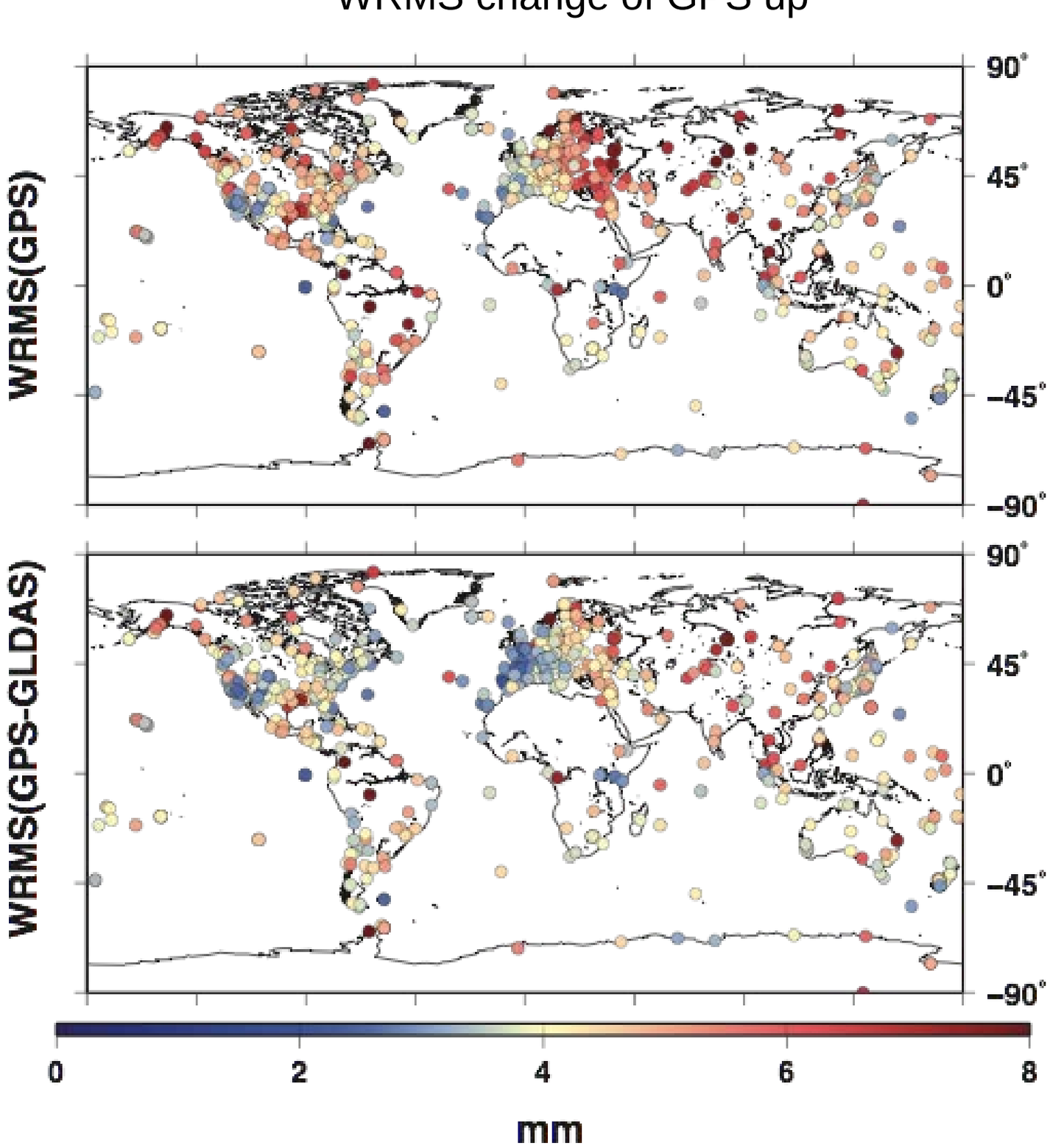

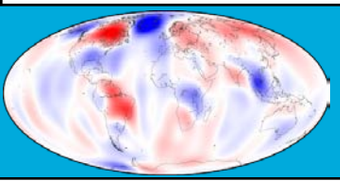

Global %ΔWRMS GPS up

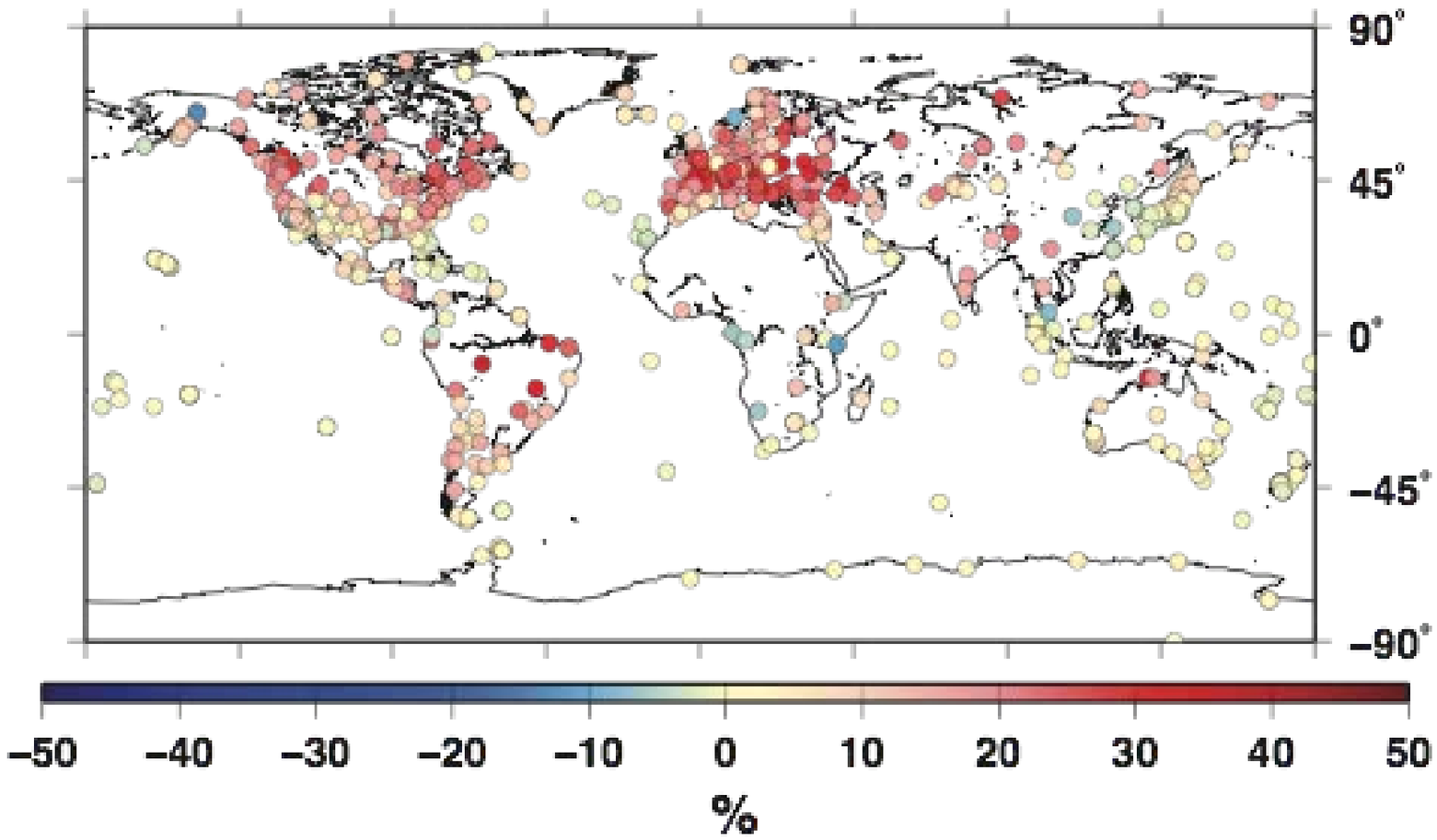

- Pink to red: stations where the WRMS of the GPS up is reduced when GLDAS correction is applied
- Blue to yellow: stations where the WMRS of the GPS up is increased => GLDAS signal adds noise to the GPS time series
- Not too many blue spots => Model does a reasonable job of removing water storage signal
- GLDAS correction is not significant at many coastal and island sites; the site's proximity to the ocean means that the water storage is low there

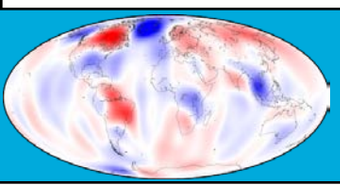

5. Non-tidal ocean loading

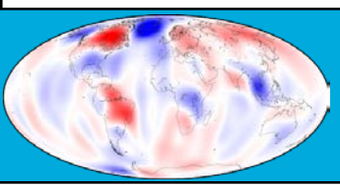

Ocean Bottom Pressure

- Ocean bottom pressure is the change in the pressure/area acting on the ocean floor
- Changes in ocean bottom pressure are driven by:
  - The internal mass redistribution of the ocean driven by ocean circulation
  - Water mass entering or leaving the ocean
    - Evaporation/Precipitation
    - Ice melt
    - River runoff
- A change in the integrated mass or air over the ocean

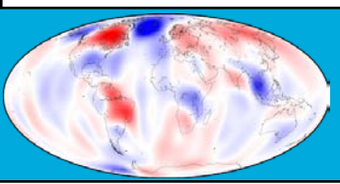

Datasets

- ECCO Estimating the Circulation and Climate of the Ocean project
  - The model assimilates altimetric sea surface heights, expendable bathythermograph (XBT) profiles, and other ocean in situ data
  - ECCO OBP is a by product of the primary product, the global circulation of the oceans
- Ocean Model for Circulation and Tides (OMCT) (*Thomas* 2002) is available from the GFZ
- OMCT and ECCO estimates of OBP are based on different models and methodologies (for more information please see *Quinn and Ponte* 2011).
- Both models agree well with each other and GRACE
- A comparison of the models with each other, GPS height time series, Ocean bottom pressure recorders shows that ECCO captures more of the OBP signal compared to OMCT. This is expected as ECCO assimilates in situ data and OMCT does not

Thomas, M. 2002) Ocean induced variations of Earth's rotation—results from a simultaneous model of global circulation and tides. PhD dissertation, University of Hamburg, Germany
Quinn KJ, Ponte RM (2011) Estimating high frequency ocean bottom pressure variability. Geophys Res Lett 38. doi:10.1029/2010GL046537

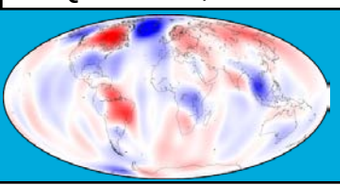

ECCO dataset

- Twice daily for the epochs 0600 and 1800 h
- Covers the latitudes between 78.5° N to 79.5° S latitude over the global oceans
- Longitudinal spacing is 1° globally
- In latitude, the spacing between the product's northern limit and 20° of the equator is 1°
- The latitudinal spacing is gradually reduced to 0.3° within 10° of the equator
- Initial processing included interpolating the data to equal spaced grids
- Initial processing also includes removing a long-term trend from the data

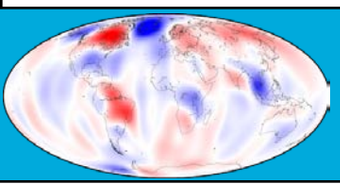

- ECCO bottom pressure data
- Figure from *Ponte et al.* (2007)
- RMS of OBP estimates in cm of equivalent water height
- Large variability in the Southern ocean
- Largest variability observed in enclosed seas or bays
- We expect the largest signal effect on the space geodetic observations to be at sites near these enclosed bays or seas

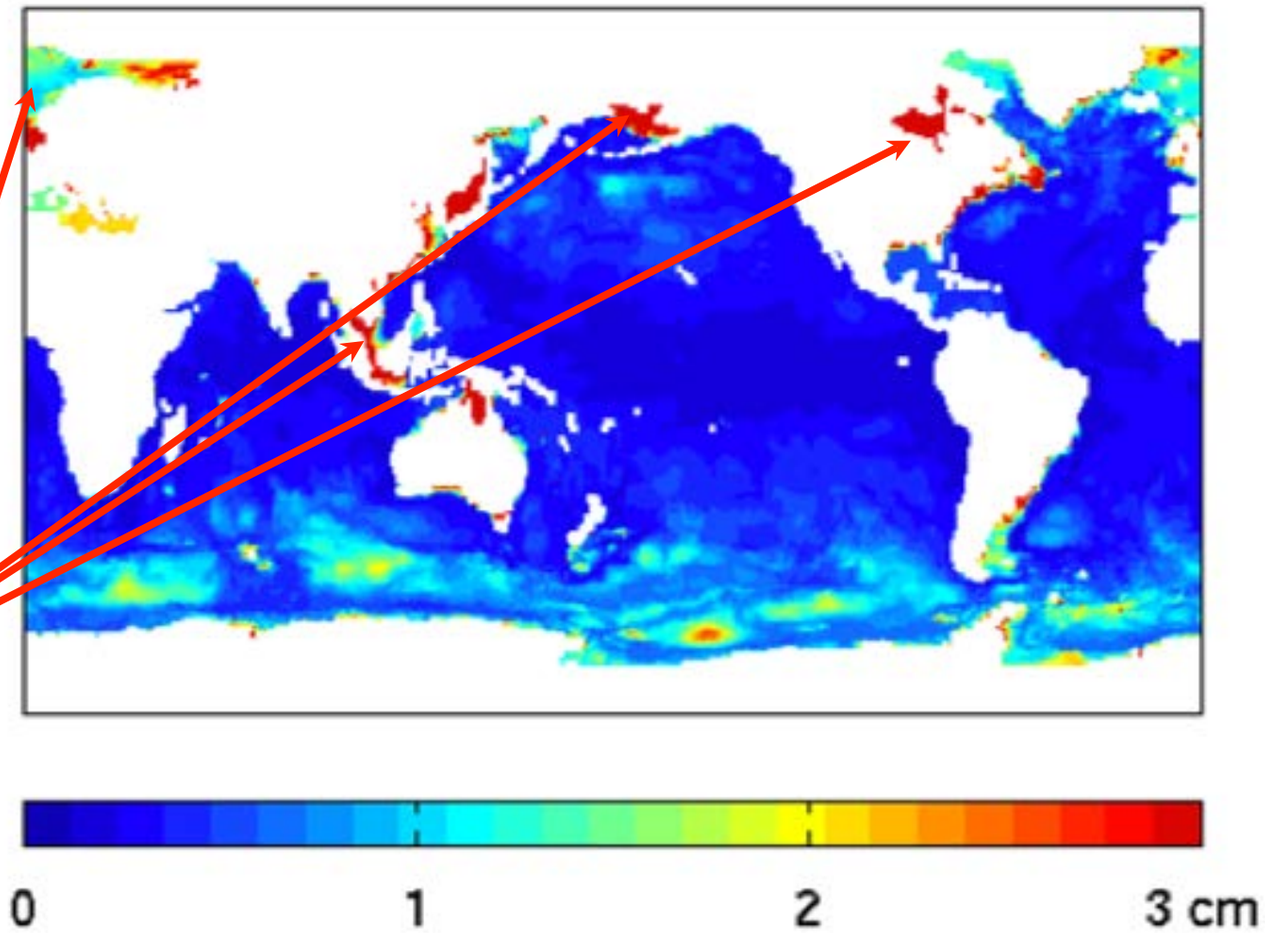

Ponte, R. M., K. J. Quinn, C. Wunsch, and P. Heimbach (2007), A comparison of model and GRACE estimates of the large-scale seasonal cycle in ocean bottom pressure, Geophys. Res. Lett., 34, L09603, doi:10.1029/ 2007GL029599.

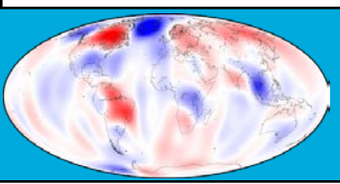

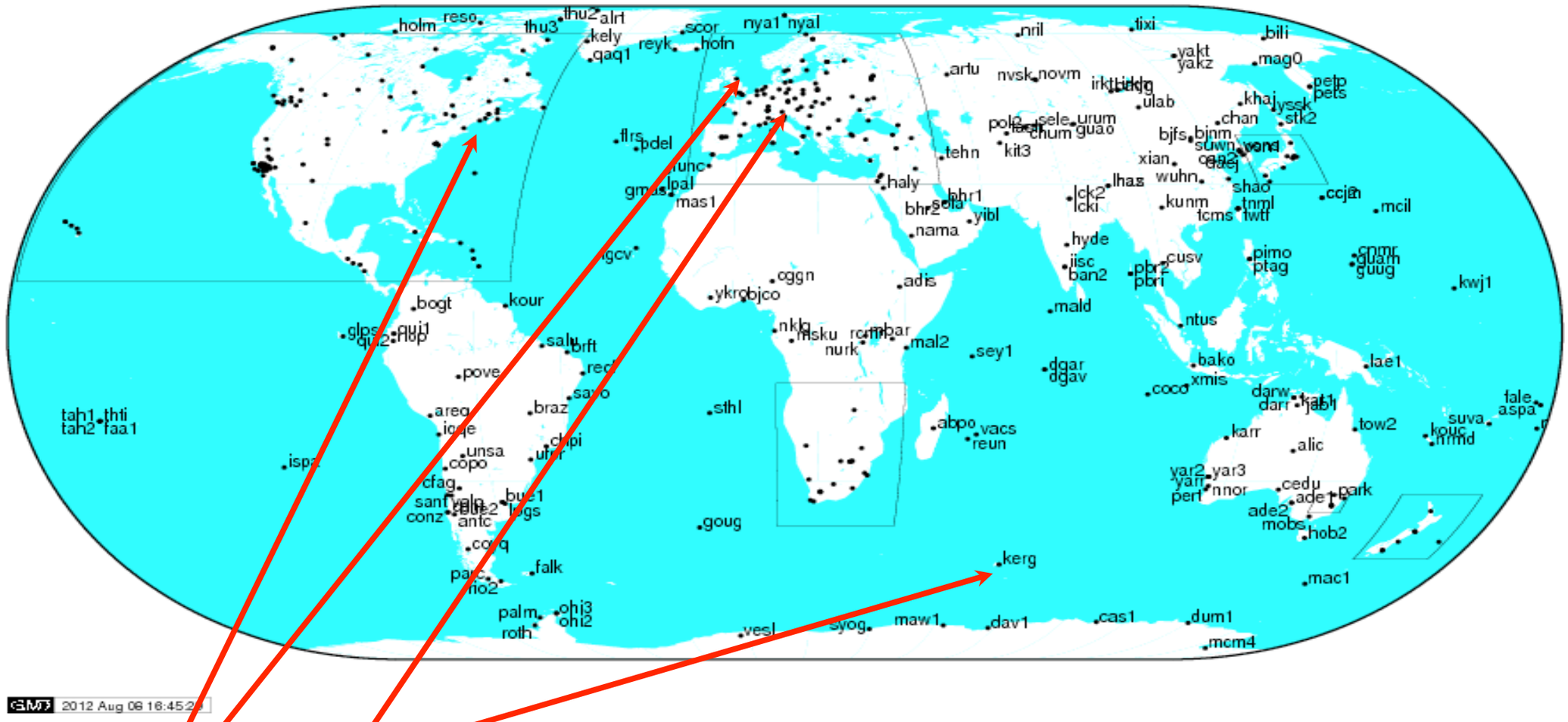

Station	Location	Longitude	Latitude
kerg	Kerguelen, France	70.26	-49.35
newl	Newlyn, United Kingdom	354.46	50.1
stjo	St. John’s New Foundland, Canada	307.32	40.65
mate	Matera, Italy (Mediterranean Sea)	16.7	40.65

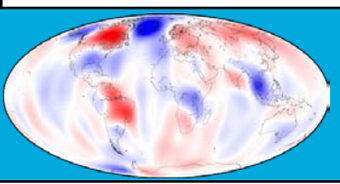

- GPS stations where the OBP signal is large, have small environmental loading due to their proximity to the coast
- OBP signal still much smaller than the GPS up
- Strong annual signal in the OBP

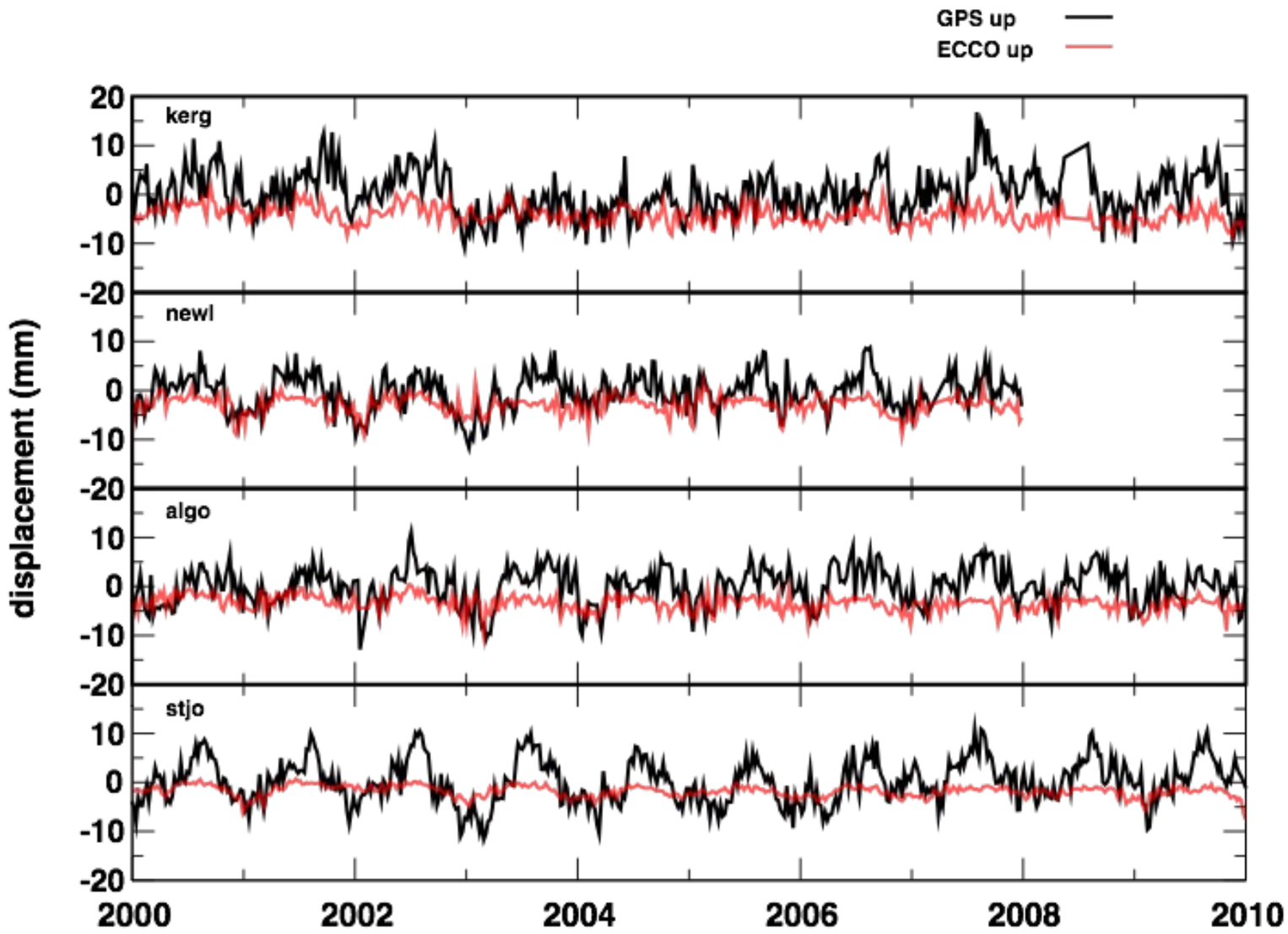

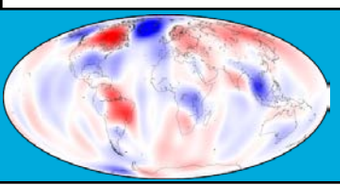

Station	WRMS(GPS) (mm)	WRMS(ECCO) (mm)	WRMS(GPS-ECCO) (mm)	%ΔWRMS
kerg	4.3	1.9	3.9	8
newl	3.6	1.8	3.1	14.1
stjo	3.6	1.6	3.1	12.5
mate	4.4	1.3	3.9	11.7

- WRMS of ECCO smaller than previous loads (ATML or CWS)
- Has a smaller impact on reducing the WRMS of the GPS up

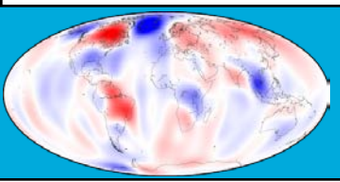

Globally?

- Top panel is the WRMS of the GPS up coordinate alone; bottom is the GPS up corrected for the OBP
- Looking for dots in the upper panel to turn from red to a lighter color or even yellow or blue in the bottom panel
- Improvement is not very clear even for stations near enclosed bays

WRMS change of GPS up

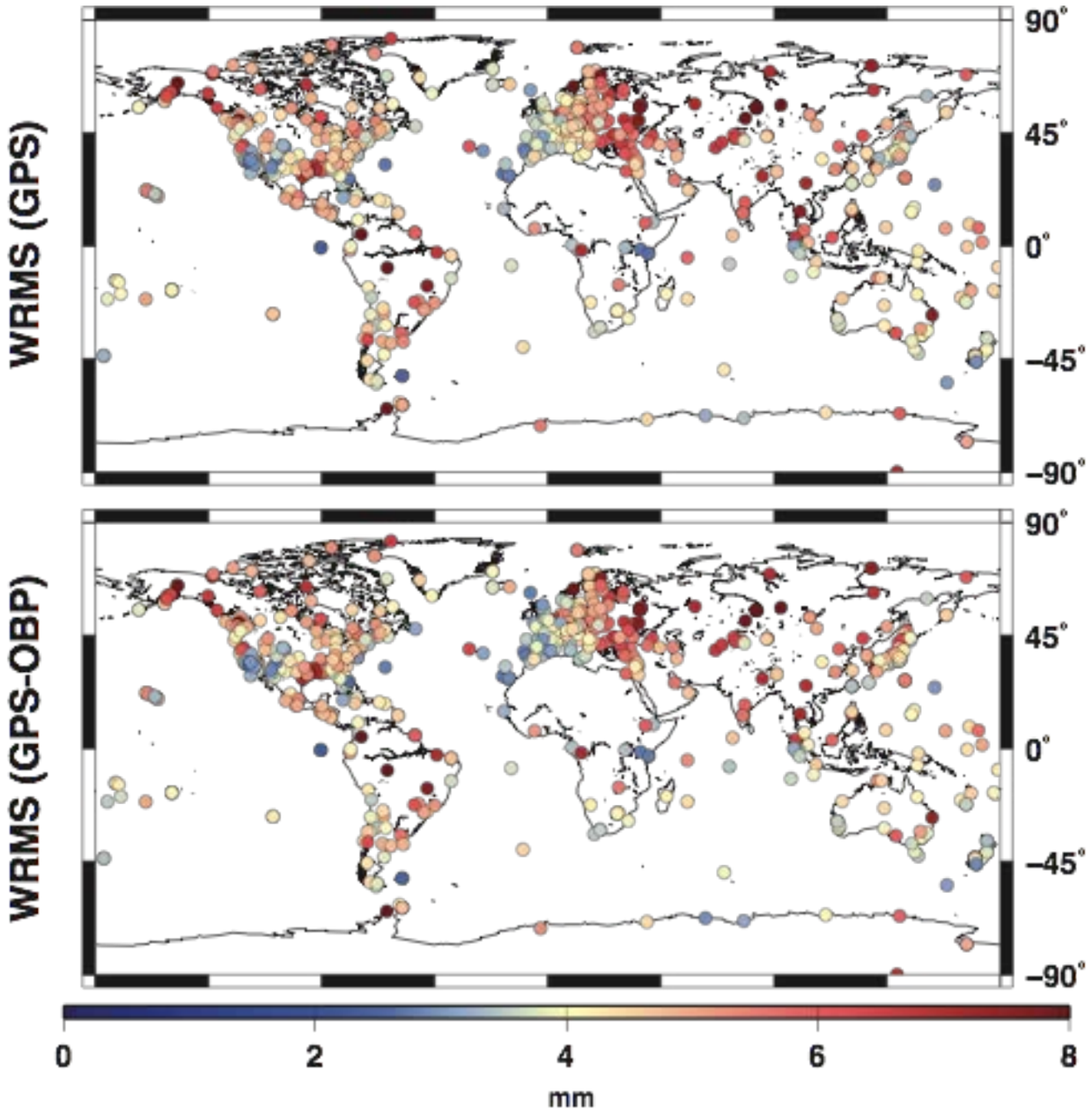

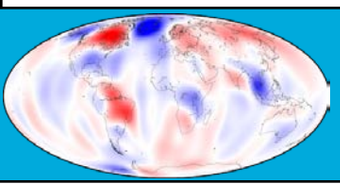

Global %ΔWRMS GPS up

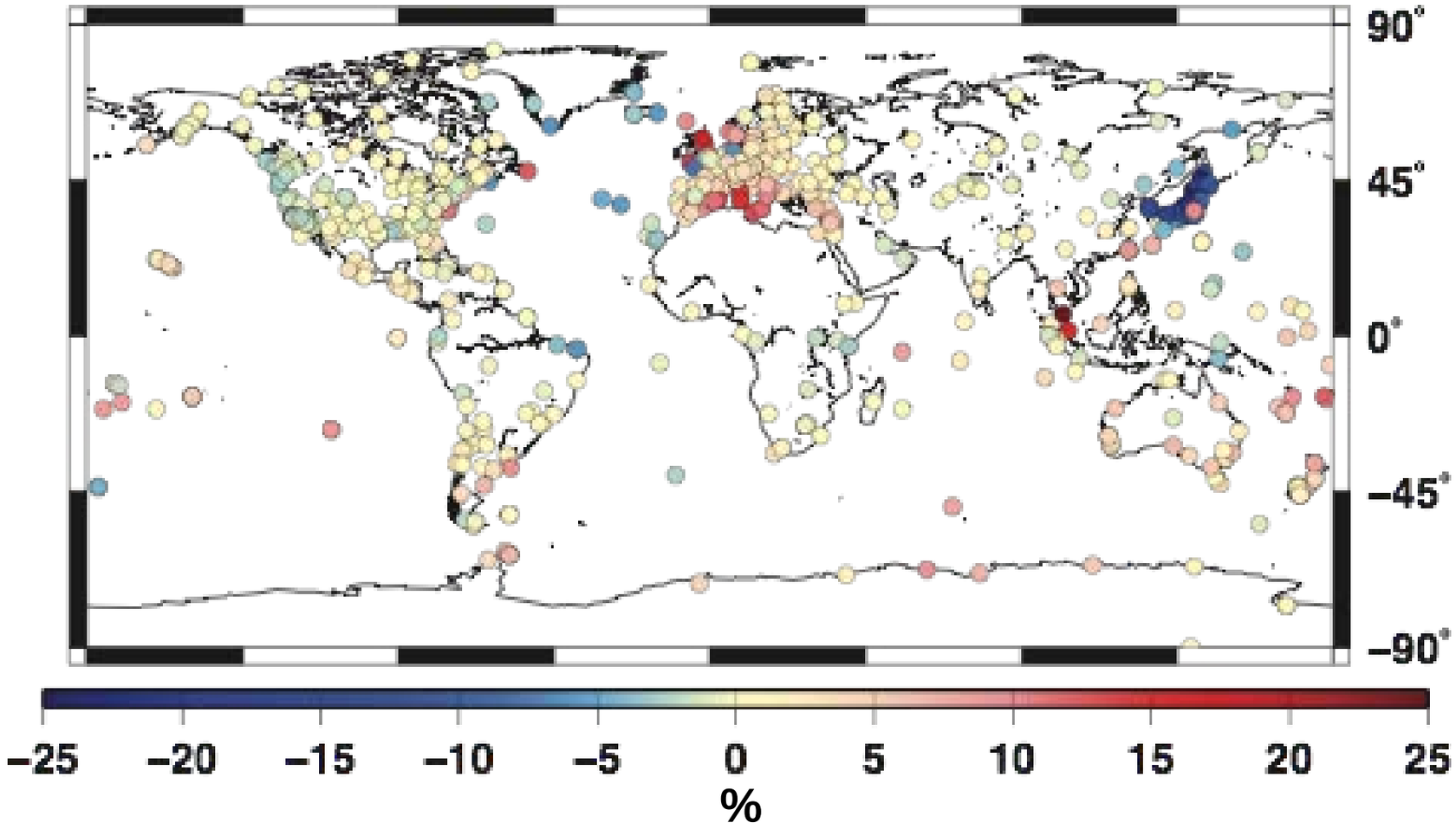

- Pink to red: stations where the WRMS of the GPS up is reduced when OBP correction is applied
- Blue to yellow: stations where the WMRS of the GPS up is increased => ECCO OBP signal adds noise to the GPS time series
- Mostly yellow dots indicating the effect is small either way
- Red dots are near enclosed bays or seas
- Not too many blue spots overall => Model does a reasonable job of removing loading effects due to OBP
- There is a problem in the Japan Sea

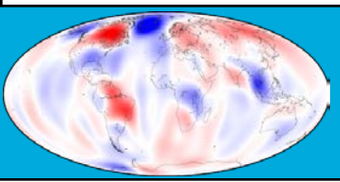

6. Estimate of the Total Loading Signal

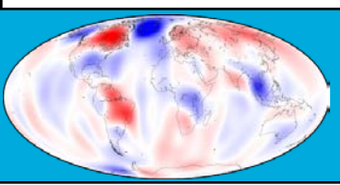

How do we get a total load model?

- So far we've been discussing individual loads from different models
- To obtain an estimate of the total load, we sum the individual components together
  - Mass is not conserved when we sum the models together
- NONETHELESS, IT IS THE BEST WE CAN DO
- Recommendations from GGFC loading workshop (2012)
  - The current solution is to sum different models.
- Total load at a site equals the sum of the individual contributions
  - NCEP
  - GLDAS
  - ECCO

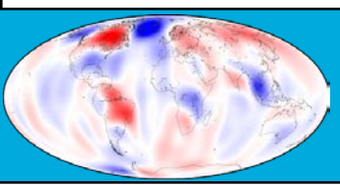

WRMS Total Load

- WRMS in mm
- Largest scatter in the North and Up found over mid to high latitudes over Asia
- Largest scatter in the East found in Europe and parts of Asia
- Smallest scatter in all coordinates near the equator
- Largest scatter almost always due to changes in continental water storage

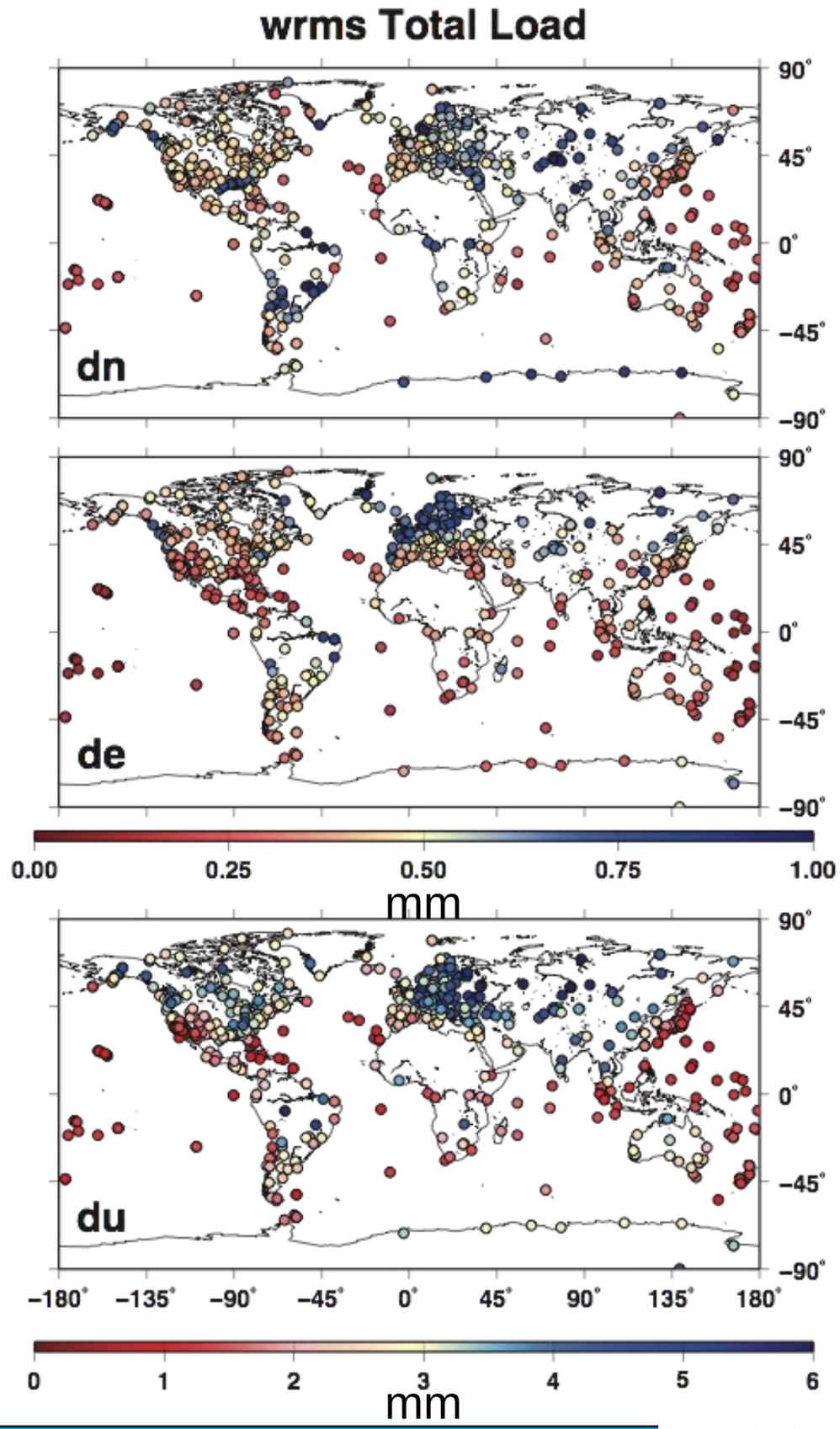

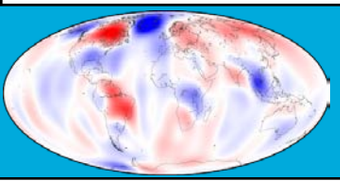

WRMS % Improvement

- Number of stations where the WRMS is reduced when the load model is applied
  - north: 495 out of 912 or 54%
  - east: 439 out of 912 or 48%
  - up: 603 out of 912 or 66%

- Biggest improvements in the mid- to high-latitudes
- Compare with the load WRMS; the largest improvement is found where the load is the largest

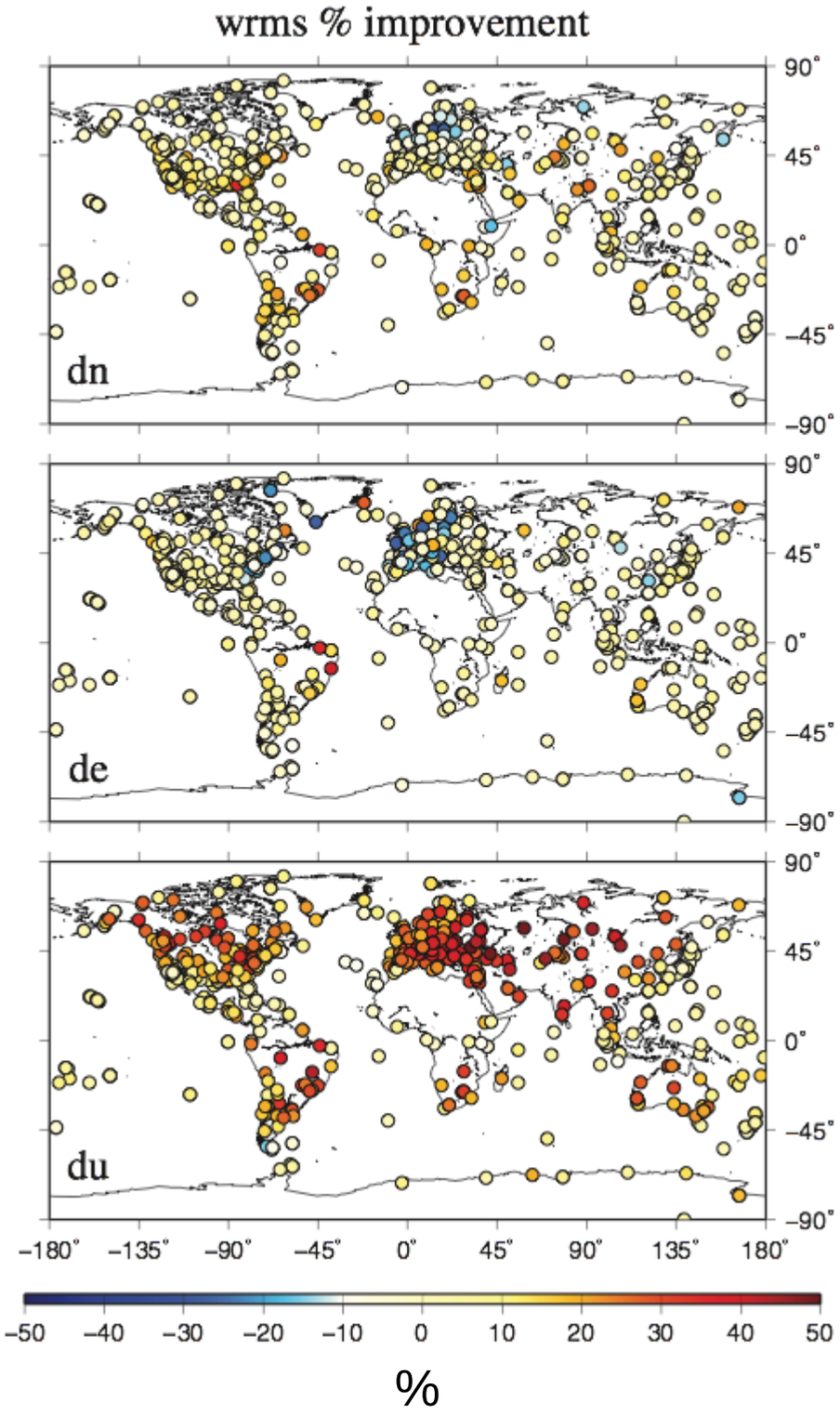

What is the amplitude of the improvement?

- Despite the fairly large number of stations where the WRMS is reduced, only a small part of the load signal is actually removed
- This is a plot showing the WRMS difference before and after the load is removed
- We see that for the horizontals, the reduction is on average 0.5 mm
- In the up, the average reduction is about 2 mm

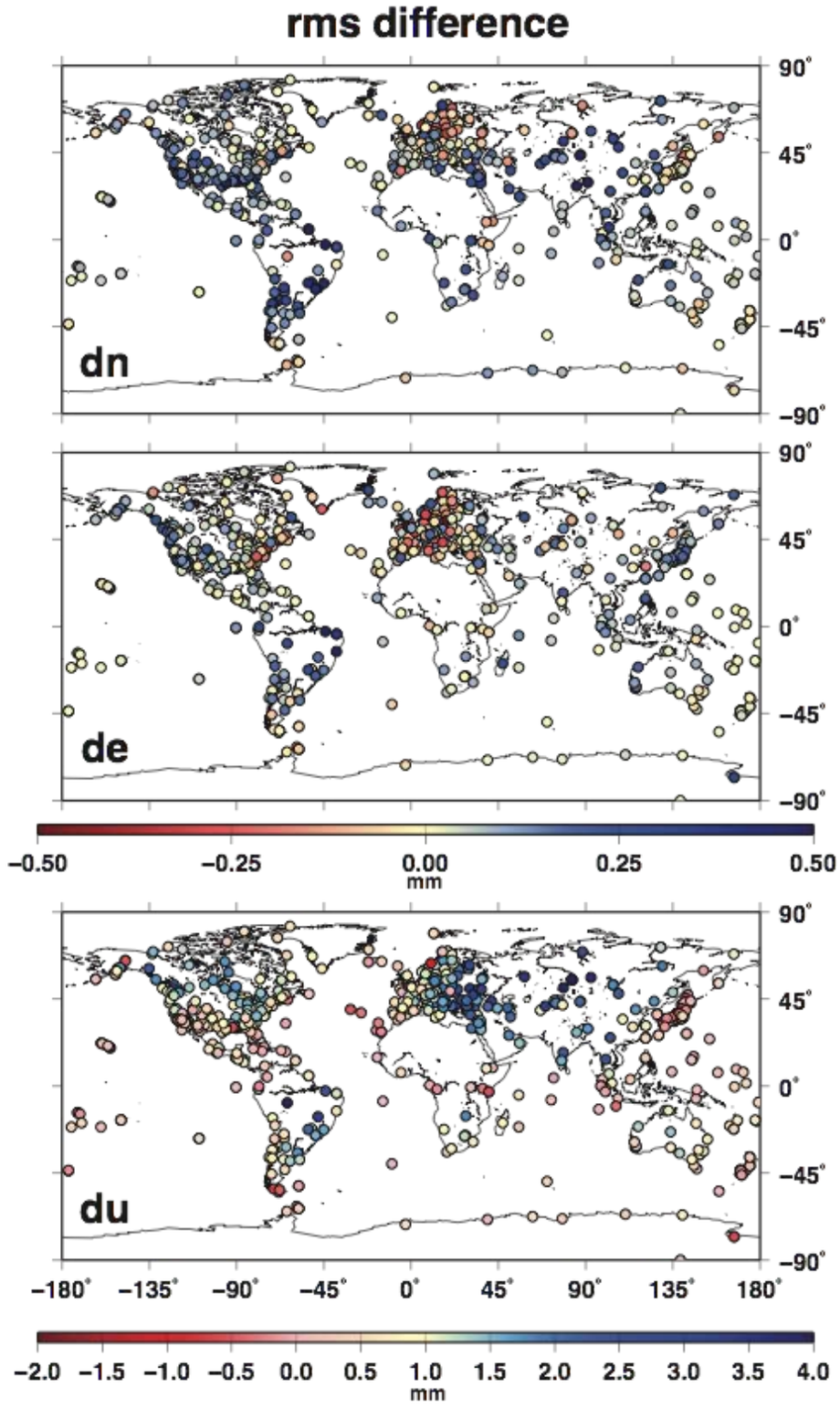

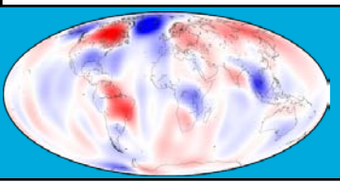

GRACE Mission

Science Goals

High resolution, mean and time variable gravity field for Earth System Science applications.

Mission Systems

Instruments

- HAIRS (JPL/SSL/APL)
- SuperSTAR (ONERA)
- Star Cameras (DTU)
- GPS Receiver (JPL)

Satellite (JPL/Astrium)
Launcher (DLR/Eurockot)
Operations (DLR/GSOC)
Science (CSR/JPL/GFZ)

Orbit

Launched: March 17, 2002
Initial Altitude: 500 km
Inclination: 89 degree
Eccentricity: ~0.001
Separation Distance: ~220 km
Nominal Mission : 5 (extended to 8) years

NASA DLR CSR JPL GFZ Potsdam

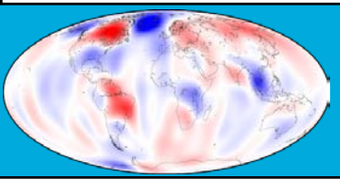

GRACE: main products

- Time-variable gravity field solutions at approximately monthly intervals
- Static mean gravity fields (e.g., GGM01C, GGM02C, …)
- In forms of fully normalized spherical harmonics (or Stokes coefficients) up to degree and order 60 or 90 (for time-variable fields).
- From three official processing centers: CSR, GFZ, and JPL and other institutions like GRGS, Uni Bern and TU Graz
- Supporting data products
  - GAC (combination of atmospheric and oceanic de-aliasing products),
  - GAB (oceanic de-aliasing products)
  - GAA (atmospheric de-aliasing products)
  - and etc

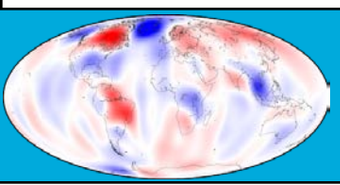

Comparison between GPS and GRACE

- Standard Monthly GRACE fields post-processing when comparing with GPS

	GFZ RL05a, CSR RL05, JPL RL05, AIUB RL02, ITSG2016, EGSIEM (combined)	GRGS RL03
• replace C20 from SLR	X	-
• restoring degree-1 from Swenson	X	-
• applying filtering of Gaussian 500	X	-
• adding back GAC product removed during de-aliasing	X	X
• fit & remove mean & trend	X	X
• displacement in CF using spherical harmonic approach	X	X

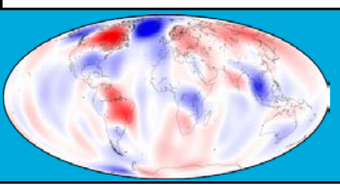

Comparison between GPS and GRACE

- Comparing GRACE-derived displacements with GPS-observed deformation (monthly averaged ITRF2014 residuals, IGN) at vertical component using different GRACE products.

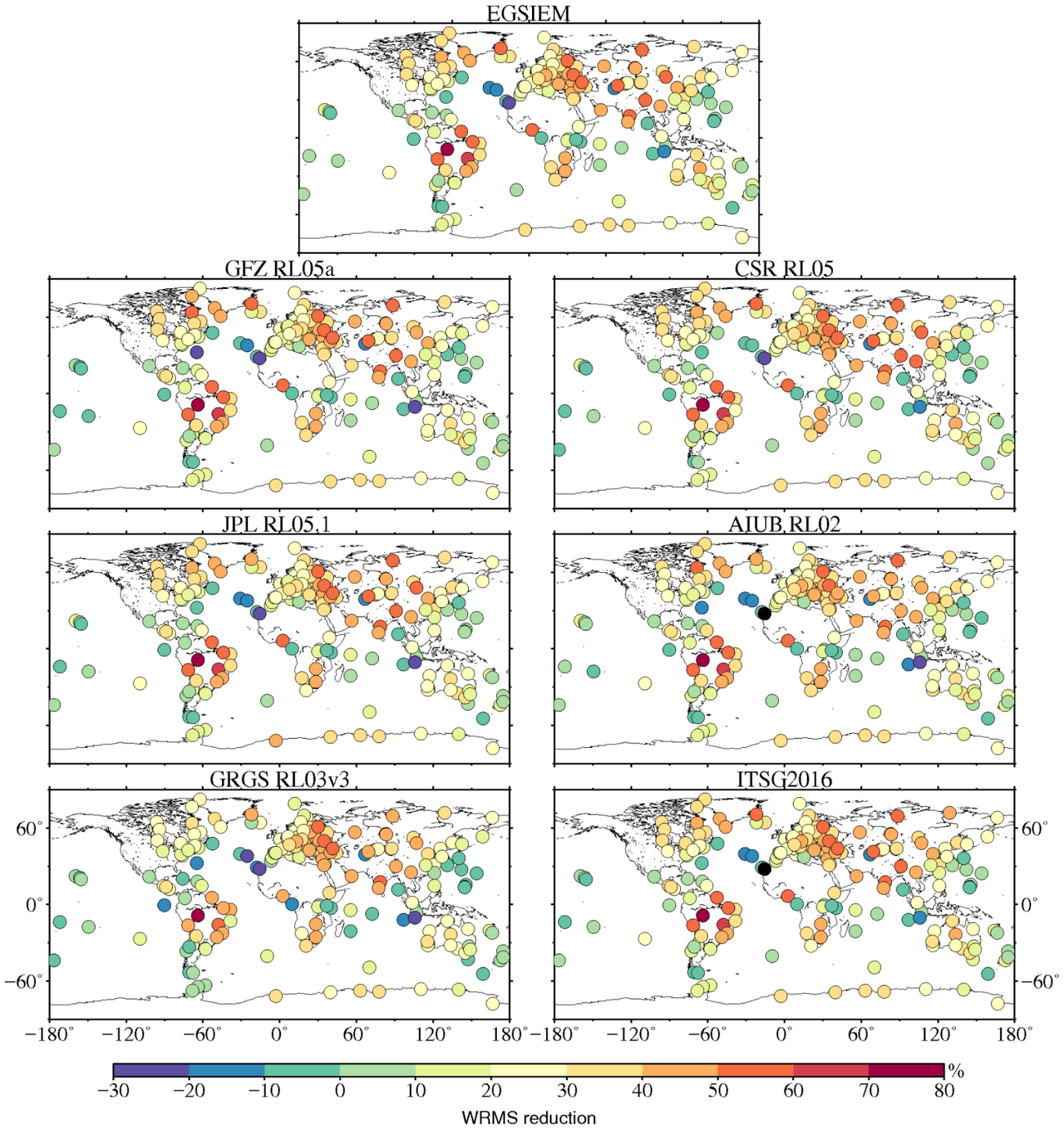

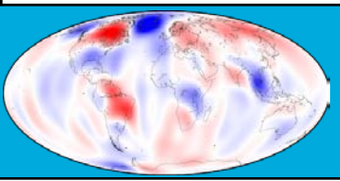

Take home messages

- Environmental loading, e.g. atmosphere, ocean and continental water, loads and deforms the Earth's crust elastically.
- Green's functions approach (spatial convolution) and spherical harmonic approach (spectral convolution) can be used to compute the displacements due to various environmental loading.
- Existing environmental models do a reasonable job of predicting the surface displacements due to the redistribution of environmental mass.
- GRACE products can serve as total load and its derived displacements provide good agreements with GPS-observed deformations.

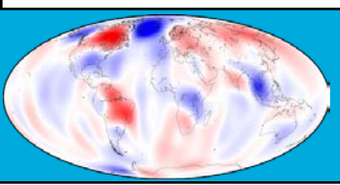

Back-up slides

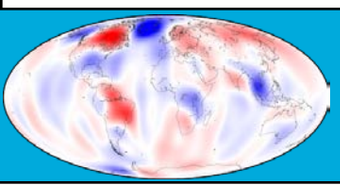

Green's functions from Farrell

- Table A3, Farrell (1972)

TABLE A3. Mass-Loading Green's Functions, G-B Earth Model
(Applied load, 1 kg.)

θ, deg	Radial Displacement, $\times 10^{12}(a\theta)$	Tangential Displacement, $\times 10^{12}(a\theta)$	g^E, $\times 10^{18}(a\theta)$	t^E, $\times 10^{12}(a\theta)^2$	$\epsilon_{\theta\theta}$, $\times 10^{12}(a\theta)^2$
0.0001	−33.64	−11.25	−77.87	33.64	11.248
0.0010	−33.56	−11.25	−77.69	33.64	11.248
0.0100	−32.75	−11.24	−75.92	33.64	11.253
0.0200	−31.86	−11.21	−73.96	33.62	11.278
0.0300	−30.98	−11.16	−72.02	33.58	11.322
0.0400	−30.12	−11.09	−70.11	33.52	11.382
0.0600	−28.44	−10.90	−66.40	33.30	11.537
0.0800	−26.87	−10.65	−62.90	32.92	11.709
0.1000	−25.41	−10.36	−59.64	32.35	11.866
0.1600	−21.80	−9.368	−51.47	29.82	11.988
0.2000	−20.02	−8.723	−47.33	27.78	11.714
0.2500	−18.36	−8.024	−43.36	25.29	11.083
0.3000	−17.18	−7.467	−40 44	23 09	10.303
0.4000	−15.71	−6.725	−36 61	19.84	8.779
0.5000	−14.91	−6.333	−34.32	17.85	7.538
0.6000	−14.41	−6.150	−32.78	16.81	6.682
0.8000	−13.69	−6.050	−30.59	16.25	6.019
1.0	−13.01	−5.997	−28.75	16.32	6.170
1.2	−12.31	−5.881	−27.03	16.33	6.535
1.6	−10.95	−5.475	−23.96	15.86	7.071

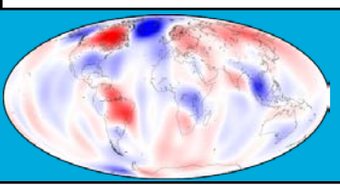

Green's functions from Farrell

- Table A3, Farrell (1972)

TABLE A3. (continued)

θ, deg	Radial Displacement, $\times 10^{12}(a\theta)$	Tangential Displacement, $\times 10^{12}(a\theta)$	g^E, $\times 10^{18}(a\theta)$	t^E, $\times 10^{12}(a\theta)^2$	$\epsilon_{\theta\theta}$, $\times 10^{12}(a\theta)^2$
2.0	−9.757	−4.981	−21.38	14 95	7.114
2.5	−8.519	−4.388	−18.74	13.68	6.830
3.0	−7.533	−3.868	−16.64	12.38	6.332
4.0	−6.131	−3.068	−13.59	10.09	5.261
5.0	−5.237	−2.523	−11.55	8.27	4.297
6.0	−4.660	−2.156	−10.16	6.90	3.445
7.0	−4.272	−1.915	−9.169	5.94	2.765
8.0	−3.999	−1.754	−8.425	5.23	2.230
9.0	−3.798	−1.649	−7.848	4.72	1.800
10.0	−3.640	−1.582	−7.379	4.38	1.485
12.0	−3.392	−1.504	−6.638	3.93	1.122
16.0	−2.999	−1.435	−5.566	3.52	0.788
20.0	−2.619	−1.386	−4.725	3.36	0.712
25.0	−2.103	−1.312	−3.804	3.31	0.812
30.0	−1.530	−1.211	−2.951	3.29	1.104
40 0	−0.292	−0.926	−1.427	2.94	2.040
50.0	0.848	−0.592	−0.279	1.94	2.928
60.0	1.676	−0.326	0.379	0.39	3.253
70.0	2.083	−0.223	0.557	−1.25	2.829
80.0	2.057	−0.310	0.353	−2.71	1.789
90.0	1.643	−0.555	−0.110	−3.76	0.395
100.0	0.920	−0.894	−0.713	−4.31	−1.094
110.0	−0.025	−1.247	−1.357	−4.39	−2.475
120.0	−1.112	−1.537	−1.980	−4.18	−3.656
130.0	−2.261	−1.706	−2.557	−3.72	−4.638
140.0	−3.405	−1.713	−3.076	−3.12	−5.473
150.0	−4.476	−1.540	−3.530	−2.44	−6.191
160.0	−5.414	−1.182	−3.918	−1.67	−6.825
170.0	−6.161	−0.657	−4.243	−0.83	−7.441
180.0	−6 663	0	−4.514	0	−8.203

mks units throughout. The normalizations (a = earth's radius, 6.371×10^6 m, θ = distance from load in radians) are convenient scalings that facilitate intercomparisons. For this model, $\lambda(a)/\sigma(a) = 0.3311$.